



NTNU – Trondheim
Norwegian University of
Science and Technology

Experimental Study of CO₂ Solubility in Ionic Liquids and Polyethylene Glycols

Huang Huang

Chemical Engineering

Submission date: July 2015

Supervisor: Liyuan Deng, IKP

Norwegian University of Science and Technology
Department of Chemical Engineering



Faculty of Natural Science
Department of Chemical Engineering

TKP4900 - Thesis

**Experimental Study of CO₂ Solubility in
Ionic Liquids and Polyethylene Glycols**

Written By:

Huang (Patrick) HUANG

Supervisors:

A/Prof. Liyuan Deng

PhD Muhammad Usman

Acknowledgement

First and foremost, I would like to express my sincere gratitude to the supervisor of this project, **Associate Professor Liyuan Deng**, for her patient guidance, enlightening criticism, and kind encouragement during this working period. Also I really appreciate Professor Deng's key material provided that related to the project.

I would also like to extend my sincere thanks to co-supervisor **PhD Muhammad Usman**. In this semester, Mr. Usman gave me great help, from the basic experimental training to his newest research focus. Without his selfless support and clear tutorial, I will have much more difficulties for understanding the relevant background information.

Furthermore my appreciation is also for **Professor May-Britt Hägg, PhD Zhongde Dai, Dr. Xuezhong He, Dr. Arne Lindbråthen, Dr. Mikael Hammer, Dr. Luca Ansaloni, PhD Muhammad Saeed, Ms. Gunn Torill Wikdahl** and **Ms. Gøril Flatberg**. Honestly, it is my fortunate to work with them for the whole semester.

My special thanks are for **Norwegian University of Science and Technology (NTNU)**, and **University of New South Wales (UNSW)**, my home university. I am so grateful for having this valuable exchange year, and finish my thesis in such an excellent environment.

Abstract

In the recent years, the issue of environment protection gradually attracts more and more attention, with sustainable development becomes the consensus of human beings. However, the serious emission of carbon dioxide is considered as a huge obstruction of this goal, thus various methods of carbon capture and storage (CCS) turn into one of the research focus. Currently, only traditional absorbents are widely used in industrial applications, and their performance under actual conditions is not satisfied. Hence, researching and developing new carbon capture absorbents comes to be meaningful in this aspect.

After a detailed literature review of previous absorption research, this thesis puts forward the further research of tetrabutylphosphonium glycine ($P_{4444}\text{Gly}$) mixing with polyethylene glycol with average molecular weight 400 (PEG400) as a co-solvent, in order to find out the most reasonable mixing ratio of blend and absorption-desorption temperatures of this system.

The thesis includes synthesis of $P_{4444}\text{Gly}$ in the evaluation. Besides, in order to assess the performance of $P_{4444}\text{Gly}$ -PEG400 system, a series of experiments are designed for measuring the density and viscosity of all those samples. According to those experiments, the synthesis of $P_{4444}\text{Gly}$ is generally reliable but the possible production amount is still low per production, indicates a further optimisation is beneficial. The density is tested in 20-80 °C and the viscosity is tested at 25-120 °C. Those properties are in reasonable ranges and therefore assumed to be an acceptable combination.

The CO_2 absorption and desorption experiments are also designed for up to pressure up to 18 bar at 60-140 °C. Comprehensively speaking, 0.5 $P_{4444}\text{Gly}$ -0.5PEG are suggested because of its highest cost effective, with 60 °C in absorption and 120 °C in desorption as the best temperature in the selected range. The Henry's constant ranges from 1.63-10.77 MPa, considered as a generally good solvent with the comparison. For cyclic capacity test of $P_{4444}\text{Gly}$ -PEG400, the first cycle gets a good effect but not the following cycles, which mainly because the chemical absorption is not reversible under the designed conditions. Several observations were taken during the experimentation such as, the solution may deteriorate at high temperature, that is probably because of thermal decomposition of the solvent or reaction with absorption vessel.

Table of content

1. Introduction and Background Information	1
1.1. Environmental Impact and Carbon Capture	1
1.2. Project Design Concept	3
1.3. Project Objective	4
2. Literature Review	5
2.1. Ionic Liquid Absorption Method	5
2.2. Absorption of Ionic Liquid with PEG as Co-solvent	8
3. Materials and Methods	10
3.1. Synthesis of P4444Gly	10
3.1.1. Chemical Information	10
3.1.2. Procedure of Synthesis	11
3.1.3. Purity Testing by NMR	12
3.2. Density Measurement	13
3.3. Viscosity Measurement	14
3.4. Solubility Measurement	16
3.5. Simulation and Calculation of CO ₂ Solubility	18
3.6. Calculation of Henry's Constant	20
4. Results and Analysis	22
4.1. P4444Gly Synthesis	22
4.2. Density Measurements	24
4.3. Viscosity Measurement	27
4.4. CO ₂ Absorption and Desorption by Chemical	30
4.4.1. Absorption and Desorption of Pure PEG400	30
4.4.2. Absorption and Desorption of Pure P4444Gly	33
4.4.3. Absorption and Desorption of 0.3P4444Gly-0.7PEG400	36
4.4.4. Absorption and Desorption of 0.5P4444Gly-0.5PEG400	39
4.4.5. Absorption and Desorption of 0.7P4444Gly-0.3PEG400	41
4.5. CO ₂ Absorption and Desorption by Temperature	43
4.5.1. Absorption and Desorption at 60 °C	43
4.5.2. Absorption and Desorption at 100 °C	44
4.5.3. Absorption and Desorption at 140 °C	45
4.6. Result of Cyclic Capacity Experiment	46
4.7. Improvement and Results	48
5. Discussions and Recommendations	50
5.1. Impurities of P4444Gly	50
5.2. "Black Liquid" Issue in High Temperatures	51
5.3. Comparison of Henry's Constant	52
6. Conclusion	54
7. References	55
Appendices	60
Appendix I. NMR spectrometer, Bruker/Oxford DPX 400 MHz	60

Appendix II. Density meter, Anton Paar DMA 4500M	60
Appendix III. Rheometer, TA Instruments Discovery HR-2	61
Appendix IV. Evaporator	62
Appendix V. Vacuum oven	63
Appendix VI. Solubility of CO ₂ in PEGs	64
Appendix VII. CO ₂ calculation by Aspen Plus V8.2, simulator part	64
Appendix VIII. Various NMR result graphs	65
Appendix IX. CO ₂ calculation by Aspen Plus V8.2, result page	66
Appendix X. Density of PEG400, P4444Gly and their blends	66
Appendix XI. Density comparison of PEG400	67
Appendix XII. Viscosity data of PEG400 and 0.3P4444Gly-0.7PEG400	67
Appendix XIII. Comparison of PEG400 viscosity	67
Appendix XIV. Viscosity difference between this rheometer and reference	68
Appendix XV. Experimental Values of Mole Fraction and Molality of CO ₂ in PEG400 at Equilibrium Pressure and Temperature	69
Appendix XVI. CO ₂ desorption data at 60 °C	70
Appendix XVII. CO ₂ desorption data at 100 °C	70
Appendix XVIII. CO ₂ desorption data at 140 °C	71

Lists of symbols

Symbols	Descriptions
P	Pressure
V	Volume
T	Temperature
R	Gas constant
n	Molar number
ρ	Density
m	Mass
η	Viscosity
P_g	Gas pressure
P_e	Equilibrium pressure
n_g	Gas molar number
n_e	Equilibrium molar number
He	Henry's constant
x	Molar fraction of solubility
P_c	Pressure at critical point
T_c	Temperature at critical point

Symbols	Units	Descriptions
$^{\circ}\text{C}$	Degree celsius	Temperature
Pa	Pascal	Pressure
bar	10^5 Pascal	Pressure
kPa	Kilopascal	Pressure
mPa	Millipascal	Pressure
cm	Centimetre	Length
g	Gram	Mass
s	Second	Time
δ	ppm	Chemical displacement

List of Figures

Figure 1.1. Various technology options for CO ₂ capture and separation with description of sub-techniques.	2
Figure 2.1. Chemical structures of various ionic liquids	5
Figure 2.2. Structural formula of P ₄₄₄₄ Gly	6
Figure 2.3. Mechanism of CO ₂ absorption and desorption of P ₄₄₄₄ Gly	6
Figure 2.4. Solubility of CO ₂ in PEGs	9
Figure 3.1. Result page of rheometer program	14
Figure 3.2. Solubility apparatus	16
Figure 3.3. Main screen of CO ₂ calculation, by Aspen Plus V8.2	18
Figure 4.1. IR spectrum of P ₄₄₄₄ Gly from NMR	22
Figure 4.2. Density of P ₄₄₄₄ Gly, PEG400 and their blends	24
Figure 4.3. Comparison of PEG400 density	25
Figure 4.4. Comparison of PEG400 viscosity	28
Figure 4.5. CO ₂ absorption and desorption of PEG400	30
Figure 4.6. CO ₂ absorption of PEG400 compare with literature data	31
Figure 4.7. Comparison of PEG400 before experiment and after the experiment at 140 °C	32
Figure 4.8. CO ₂ absorption and desorption of P ₄₄₄₄ Gly	33
Figure 4.9. Screenshot of P ₄₄₄₄ Gly absorption in low pressure	34
Figure 4.10. Comparison of P ₄₄₄₄ Gly before experiment, after 60 °C absorption and after 100 °C absorption	34
Figure 4.11. CO ₂ absorption and desorption of 0.3P ₄₄₄₄ Gly-0.7PEG400	36
Figure 4.12. CO ₂ absorption of 0.3P ₄₄₄₄ Gly-0.7PEG400 compare with literature data	37
Figure 4.13. shows the original mixture and the collected sample after those three experiments.	38
Figure 4.14. CO ₂ absorption and desorption of 0.5P ₄₄₄₄ Gly-0.5PEG400	39
Figure 4.15. Comparison of 0.5P ₄₄₄₄ Gly-0.5PEG400 before experiment, after 60 °C, 100 °C and 140 °C experiment	40
Figure 4.16. CO ₂ absorption and desorption of 0.7P ₄₄₄₄ Gly-0.3PEG400	41
Figure 4.17. Comparison of 0.7P ₄₄₄₄ Gly-0.3PEG400 before experiment, after 60 °C, 100 °C and 140 °C experiment	42
Figure 4.18. CO ₂ absorption data at 60 °C	43
Figure 4.19. CO ₂ absorption data at 100 °C	44
Figure 4.20. CO ₂ absorption data at 140 °C	45
Figure 4.21. Cyclic capacity experiment of 0.3P ₄₄₄₄ Gly-0.7PEG400	46
Figure 4.22. Comparison of 0.3P ₄₄₄₄ Gly-0.7PEG400 before experiment, after 60 °C, 140 °C, and cyclic capacity experiment	47
Figure 4.23. Additional experiment data of 0.7P ₄₄₄₄ Gly-0.3PEG400 at 120 °C and 140 °C	48
Figure 4.24. Comparison of 0.7P ₄₄₄₄ Gly-0.3PEG400 before	49

experiment, after 100 °C, 120 °C and 140 °C experiment

Figure 5.1. Slight colour difference between different samples 50

Figure 5.2. An comparison of produced 0.5P₄₄₄₄Gly-0.5PEG400 before 51
experiment, after 140 °C experiment for 14 hours and after 140 °C
experiment for 4-5 days

List of Tables

Table 1.1. Molar, temperature and pressure range of this work	4
Table 3.1. Chemical information of this work	10
Table 3.2. Henry's constants (bar) for gases in various organic compounds	21
Table 4.3. Viscosity comparison of standard viscosity solution for rheometer used and reference value from manufacturer	28
Table 5.1. Henry's constant of PEG400 with comparison	52
Table 5.2. Henry's constant of various P ₄₄₄ Gly-PEG400 blend	52

List of Abbreviations

Abbreviations	Full names
NTNU	Norwegian University of Science and Technology
MEMFO	Membrane Research Group
CCS	Carbon capture and storage
CO₂	Carbon dioxide
H₂O	Water (Hydrogen oxide)
D₂O	Heavy Water (Deuterium oxide)
PEG	Polyethylene glycol
PEG400	Polyethylene glycol (average molecular weight 400)
P₄₄₄₄OH	Tetrabutylphosphonium hydroxide
Gly	Glycine
P₄₄₄₄Gly	Tetrabutylphosphonium glycine
IL	Ionic liquid
NMR	Nuclear magnetic resonance
mw.	Molecular weight
wt	Weight
ppm	Parts per millions
aq.	Aqueous
CP	Chemically pure
rpm	Rounds per minute
ppm	Parts per notation

1. Introduction and Background Information

1.1. Environmental Impact and Carbon Capture

Currently, with the huge amount of fossil fuel consumption, emission of carbon dioxide (CO₂) results as a global environmental problem (Raupach et al., 2007). CO₂ is also one significant greenhouse gas and therefore causes serious global warming (D'Alessandro et al., 2010). According to the prediction of Yang et al. (2008), in order to control the temperature rise in a small amount (about 2 °C) till 2050, a 50% reduction of carbon emission should be applied.

In the heavy industry, especially the fossil fuel consuming part, there are several methods for reducing CO₂ emission. Chemical absorption method is one of the main focusing, because of its relatively new technique, flexible installation in any part of the process plant. Absorption by alkanolamine has an integral application in industry (Rochelle, 2009) and it is mainly referred by this project, but alkanolamine still has some disadvantages such as pollution and degradation etc, limits its further expansion (Veawab et al., 1999). Ionic liquids are salts of cations and anions at melting temperature lower than 100 °C. Ionic liquid has gained much attention in the recent years and capable of undetectable vapor pressure, tailored structure, high absorption capacity, high thermal and chemical stability. The tailorable structure of ionic liquid makes them to be designed for specific application. But it is also being limited by its high cost, low absorption rate and high viscosity. After further research, ionic liquids are believed to be a ideal CO₂ solvent in the future.

There are several common used methods for carbon capture and separation in chemical industry, including absorption method (Aaron & Tsouris, 2005), adsorption method (Hicks et al., 2008), cryogenic separation method (Zanganeh et al., 2009), membrane gas separation method (Bernardo et al., 2009), chemical looping combustion method (Hossain & de Lasa, 2008), microbial/algal systems (Benemann, 1997) and so on. The *Figure 1.1.* from Rao & Rubin (2002) lists several selectable methods for carbon separation.

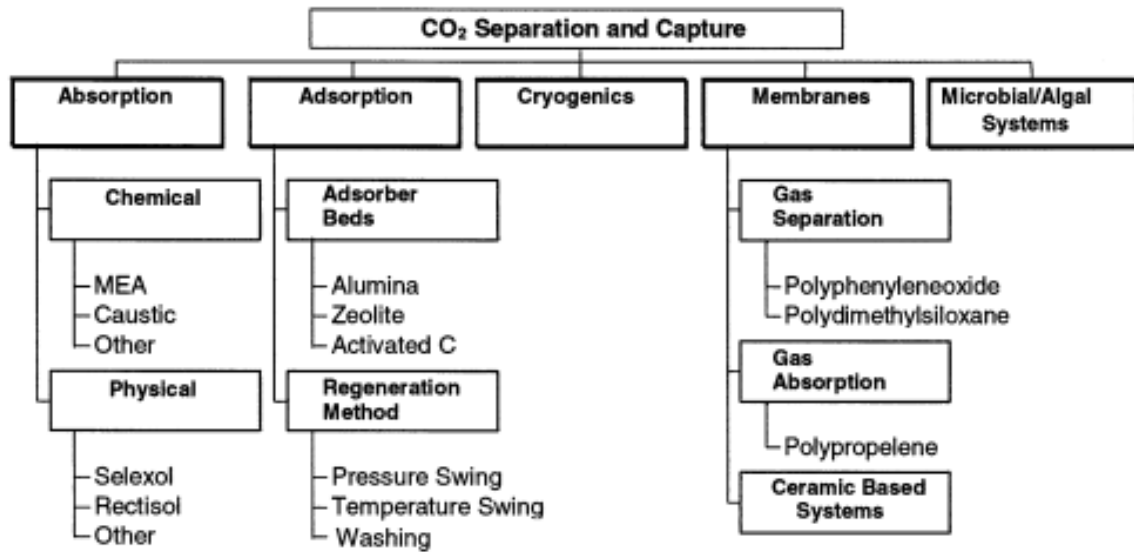


Figure 1.1. Various technology options for CO₂ capture and separation with description of sub-techniques.

Among them, the absorption method is traditional and widely used nowadays, this section will mainly introduce the mix system of PEG400 and P₄₄₄Gly, with its effect of carbon capture for a comprehensive analysis.

1.2. Project Design Concept

This project will start with a comprehensive literature review, in order to get a deep comparison of different ionic liquids, then it comes to comparison of suitable co-solvent for a mixed system. In this thesis, tetrabutylphosphonium glycine (P₄₄₄₄Gly) is chosen as the studied ionic liquid, due to the positive evaluation to it, and polyethylene glycol with average molecular weight 400 (PEG400) is selected as co-solvent.

There are very limited previous studies of this mixed system, hence, for getting more accurate results, several different mixing ratios and temperatures are chosen for finding the optimal solution. More details of experiment design are on Section 1.3., further details of review are shown in Chapter 2.

1.3. Project Objective

Based on the above description and predicted research direction, the objective of this project are:

- Trial of P₄₄₄₄Gly synthesis
- CO₂ solubility test of mixture of PEG400 and P₄₄₄₄Gly, the detail is shown in the *Table 1.1*.

Table 1.1. Molar, temperature and pressure range of this work

Component	Weight fraction					Temperature range	Pressure range
P ₄₄₄₄ Gly	100%	70%	50%	30%	0%	60 °C, 100 °C, 140 °C	Up to 18kPa
PEG400	0%	30%	50%	70%	100%		

- Density measurement of relevant P₄₄₄₄Gly-PEG400 blends.
- Viscosity measurement of relevant P₄₄₄₄Gly-PEG400 blends.
- CO₂ solubility test for cyclic capacity, absorption at 60 °C and desorption at 140 °C for 3 cycles.
- Additional experiment for possible result comparison and improving assumptions, including experiment at 40 °C and 120 °C, calculation and analysis of Henry's constant.

2. Literature Review

2.1. Ionic Liquid Absorption Method

In the past several years, research of ionic liquid gradually became a new focus of CO₂ separation (Blanchard et al., 1999). Definition of the term “ionic liquid” refers to a type of liquid that consists only ions, but excludes the ambiguity from classical meaning of molten salt (Seddon, 1997), on the contrary, it is already liquid in low temperatures (<100 °C) in this case (Wasserscheid & Keim, 2000). **Figure 2.1.** provides the structural instances of various ionic liquids.

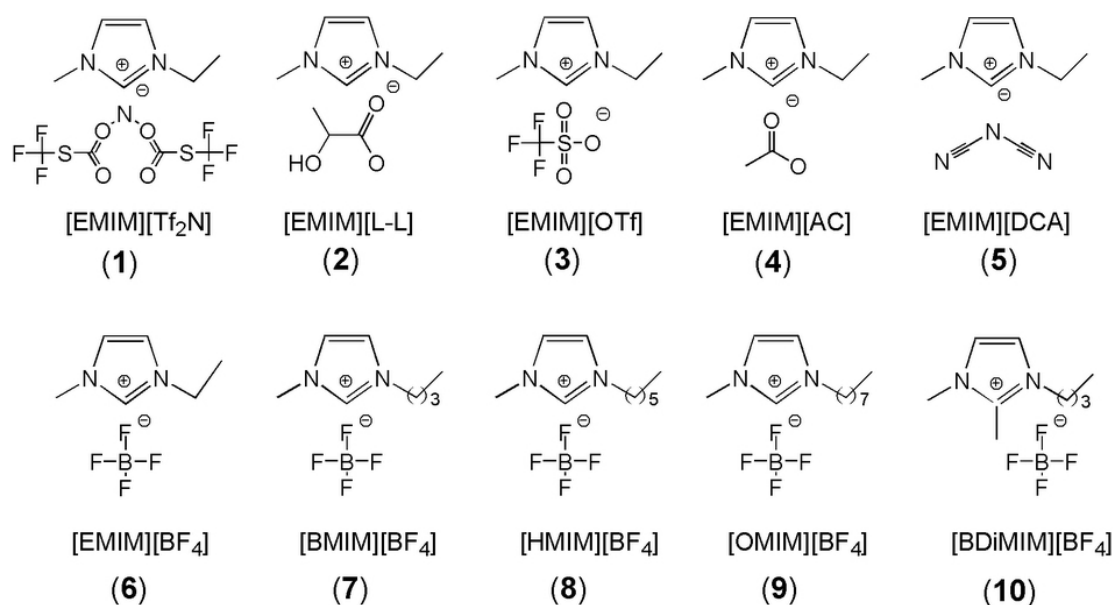


Figure 2.1. Chemical structures of various ionic liquids (Lin et al., 2013)

As a newly developed solvent, ionic liquids have several obvious advantages which attracts a lot of researches (Huang & Rüter, 2009), such as acceptable thermal stability (Rooney et al., 2010), low vapour pressure (Yoshizawa et al., 2003), low volatility (Blanchard et al., 1999), recyclable (Peng & Deng, 2001) and strong CO₂ solubility (Cadena et al., 2004). Mostly importantly, its structural flexibility gives much opportunities to “design” certain ions or functional groups for a product with specialized usage (Davis, 2004).

Although the relevant research shows the high CO₂ solubility of ionic liquids, however, those regular ionic liquids are mainly absorb CO₂ physically. The previous research of various alkanolamine (Francisco, 2006)

shows that, CO₂ has chemical contact with amine function group (-NH₂) in alkanolamine solution, that gives the inspiration of designing a new kind of functional ionic liquid which contains -NH₂. Zhang et al. (2006) had synthesized several tetrabutylphosphonium amino acid ionic liquids which fits this criteria. This work will focus on an in-depth research of one of those purposed ionic liquid, tetrabutylphosphonium glycine (P₄₄₄₄Gly). **Figure 2.2.** (Kasahara et al., 2014) presents the structural formula of P₄₄₄₄Gly.

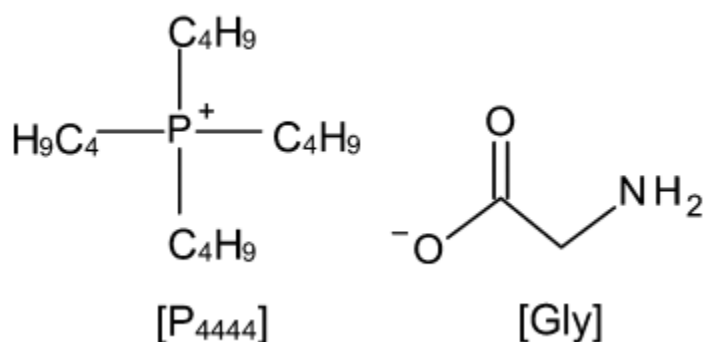


Figure 2.2. Structural formula of P₄₄₄₄Gly (Kasahara et al., 2014)

The mechanism of CO₂ absorption and desorption of P₄₄₄₄Gly are given in **Figure 2.3.** (Zhang et al., 2006) also, that shows the absorption is clearly chemical and with strong reversibility.

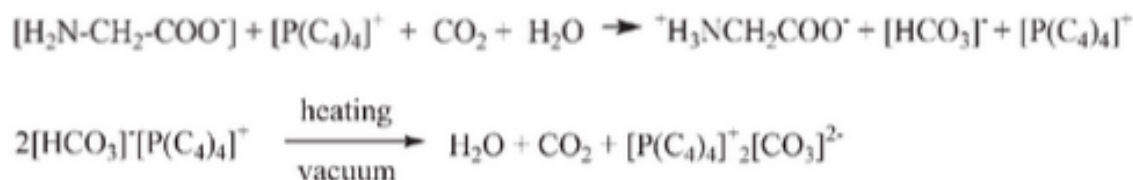


Figure 2.3. Mechanism of CO₂ absorption and desorption of P₄₄₄₄Gly

But it is still meaningful to point out that there are still several disadvantages of ionic liquids that needed to point out. Zhang et al. (2006) had research on it, but the synthesized ionic liquid has a very high viscosity, and therefore not convenient for using, and have to fix on porous membrane for further experiment. Zhang et al.'s research only repeats for four times, and that is doubtful for gaining the result with industrial meaning. High viscosity also leads to the problem of slow reaction process (Hasib-ur-Rahman et al., 2010), and the liquid might solidified or gelatinized after the experiment that brings new issues. This work had engaged the both problems, and will show and discuss the result in Section 4.4.2.

There are also concerns about toxicity (Romero et al., 2008), corrosivity (Perissi et al., 2006) and potential environmental impact during production (Li, 2014, pp.21). Further research of them is necessary for expanded usage of ionic liquid, especially for industrial purposes (Chen et al., 2007).

In this case, researchers had further experiments to mix functional ionic liquid with other solvents, such as alkanolamines (Zhang et al., 2006). Besides, PEG also gains attraction because it is also a polar solvent, therefore it has a well performance on CO₂ absorption (Li, 2014, pp.24).

2.2. Absorption of Ionic Liquid with PEG as Co-solvent

Refer to the description in Section 2.1., there are both advantages and disadvantages for adding co-solvents, a precise research and consideration is required for improving the performance of the blend system, an appropriate selection of co-solvents are useful in this regard. A possible balance is to find a kind of co-solvent that has low vapour pressure, polyethene glycols (PEGs) becomes one of the possible chemical.

PEG has several advantages that perfectly suits the requirement with great heat resistance (Want et al., 2009), low vapour pressure, non-toxic, low cost, relatively low viscosity (Han et al., 2008) and environmental friendly. The process technology of PEG is already mature and applied in several fields (Aschenbrenner & Styring, 2010).

There are different PEGs with different molecular weight, which might be considered for a better choice. According to Li (2014, pp.26), when the average molecular weight of PEG increases, the vapour pressure decreases, heat resistance increases, both of which are desired. The solubility of CO₂ also increases when average molecular weight of PEG increases (Li et al., 2011), which is shown in ***Figure 2.4***.

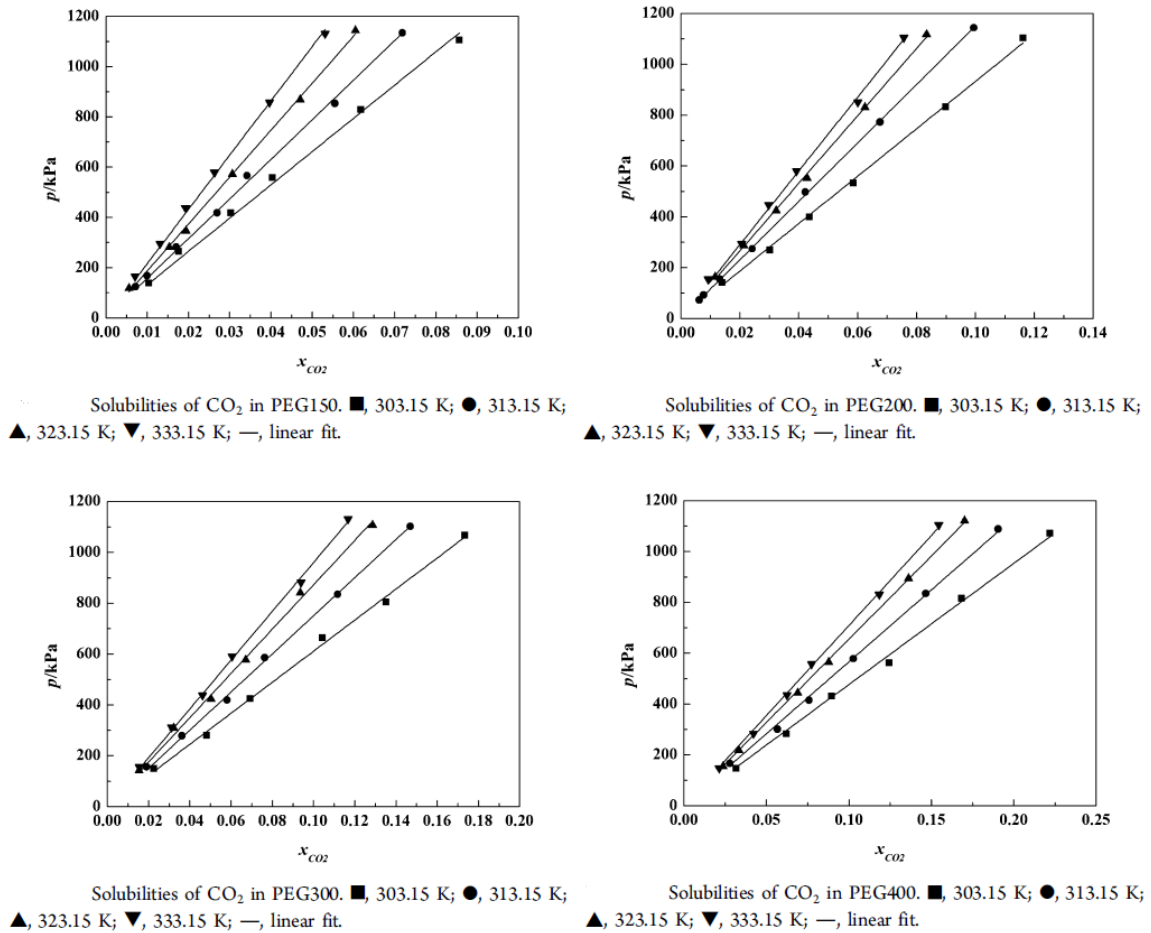


Figure 2.4. Solubility of CO₂ in PEGs (Li et al., 2011)

The viscosity of PEG also increases rapidly during this increasing, but the viscosity of the mixing system is even lower because of the decreasing of inter particle forces. However, the selection of PEG molecular weight should be controlled in a moderate extent, because the literature result (Li, 2014, pp.28) shows the blend become even more viscous when PEG600 or PEG1000 is mixing with ionic liquid, because of hydrogen bonds are forming between the composition of the blend.

As for a reasonable balance, this work will focus on the research of mix system of PEG400 and P₄₄₄₄Gly, since there is only experimental result of 0.3P₄₄₄₄Gly-0.7PEG400 (Li, 2014, pp.90), a wide-ranging research is purposed for finding a better ratio.

In addition, since the new idea is based on the result of both solubility and viscosity, an extra viscosity test is also designed for the selected mixtures, in order to gain the data which is closer to the identical result.

3. Materials and Methods

3.1. Synthesis of P₄₄₄₄Gly

There is no market-sell P₄₄₄₄Gly available, hence, synthesis of P₄₄₄₄Gly by holding chemicals is the first essential step. This section aims to describe the corresponding part including synthesis and purity testing.

3.1.1. Chemical Information

The chemical information is shown on *Table 3.1*.

Table 3.1. Chemical information of this work

Chemical	Purity	Manufacturer
P₄₄₄₄OH	40% aq. solution	Sigma-Aldrich
PEG400	Chemically pure	Sigma-Aldrich
Glycine	99% pure	Sigma-Aldrich
Methanol	99.99% pure	Sigma-Aldrich
Acetonitrile	99.99% pure	Sigma-Aldrich
Standard viscosity solution		Sigma-Aldrich
Silicone oil		Sigma-Aldrich
Carbon dioxide	99.999%	Praxair
De-ionized water		NTNU
P₄₄₄₄Gly		Product of this project

3.1.2. Procedure of Synthesis

Because P₄₄₄₄Gly is a type of ionic liquid that formed by anions and cations, it is reasonable to regard it as a salt. Therefore, the thinking of its synthesis could be the neutralization reaction by acid and alkali.

For the easiest and most economic method, this reaction is suitable to be prepared in aqueous state, but water should be fully removed during the purification process.

By this principle, the procedure of synthesis is referred from the previous reported method (Li, 2014, pp.76), and could be explained as under:

- Weight excess amount (a bit more than 3.0028g) of glycine, dissolve it in de-ionized water and stir well.
- Add 9.675g 40% wt P₄₄₄₄OH solution in glycine solution by drop wise, then stir the mixture in room temperature for 12 hours.
- Place the solution in evaporator, evaporate water at about 45 °C with vacuum, the process should last at least 4 hours.
- Mix acetonitrile and methanol with 9:1 ratio by volume, and mix again with the distilled product, for at least 4 hours.
- Filter the mixture to remove extra amino acid, then evaporated at least 4 hours to remove solvent and remaining water.
- Dry the product in vacuum oven for at least 2 days at about 70 °C, to reduce water content and volatile compounds.

Finally test the purity by NMR (Nuclear magnetic resonance) which is discussed in Section 3.1.3. Different batches of product were prepared following the same procedure.

During this step, evaporator and vacuum oven will be used, detail information and pictures of these apparatus will be shown in *Appendix IV* and *Appendix V*.

3.1.3. Purity Testing by NMR

In this part, the NMR spectrometer is used for testing purity of the product. The Bruker/Oxford DPX 400 MHz NMR spectrometer is used, a detailed figure is shown on *Appendix I*.

The sample for testing was prepared by dissolving a small amount of synthesized ionic liquid in D₂O and stir this mixture. Then it was transferred into the NMR vial by the help of a pipette. The sample was placed in the holder of NMR spectrometer and recorded the sample initials to the software of this apparatus. The proton ¹H scan was run for this sample. The result of this was a spectrum graph with different peaks. This scan was interpreted by the NMR analysis software and peak values were compared with reference from Zhang et al. (2006) to ensure the purity of the sample. The same procedure was followed for rest of the synthesized ionic liquid samples.

The result of NMR is also discussed in Section 4.1.

3.2. Density Measurement

In this project, density of all relevant samples are measured by Anton Paar DMA 4500M apparatus, which is shown in ***Appendix II***. The measuring volume is approximately 9.5ml, and the sample need to be filled in the test vial and covered by a cap (Usman, 2012). The available temperature range is set in the apparatus operating range of 20 °C to 80 °C.

Because of the temperature range is not fully suitable to the experimental temperature, some approximations are necessary, this calculation part will be discussed on Section 4.2. as well as the result.

3.3. Viscosity Measurement

The rheometer is TA Instruments Discovery HR-2, which acts as the main apparatus of viscosity measurement, is shown in *Appendix III*.

Rheometer and water bath were turned on. Water bath temperature was set to 200C. The computer program was opened. The cone type geometry was attached to the rod of the rheometer.

Firstly, rheometer was gapped zero without placing the sample on the parallel plate. The rheometer was set to lifted position. Then small amount of the sample was poured on to the parallel plate.

The amount of sample being used for the test was 1.25 ml as suggested by the software according to the geometry type. The required temperature was set and flow-sweep method was used for viscosity measurements. The rheometer was set to the measuring position and a plot representing shear rate on x-axis and shear stress on the y-axis was obtained after the run as shown in the *Figure 3.1*. This plot was analyzed for Newtonian method and got the viscosity value of the measuring sample. The same procedure was followed for rest of the samples.

The geometry used for the measurements is cone type with angle of 1 ° degree.

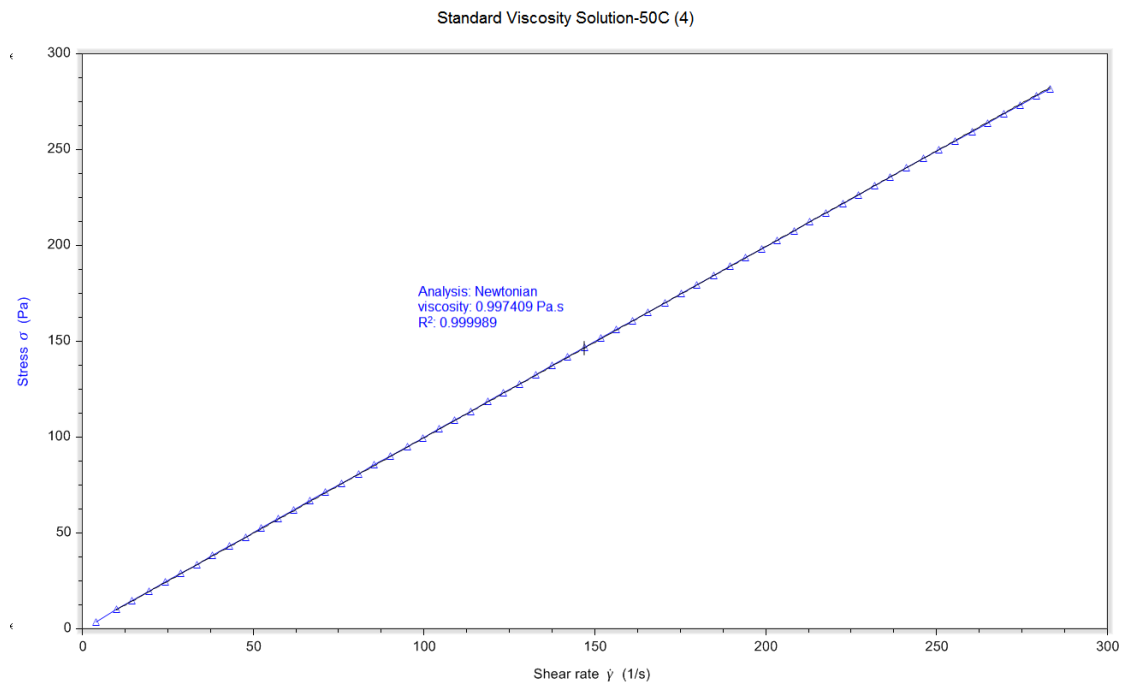


Figure 3.1. Result page of rheometer program

The above is one example of the program. The shear rate and stress are measured and shown in x and y axis, the gradient will be viscosity after an auto calculation of the program.

The result of viscosity experiment will be discussed on section 4.3.

3.4. Solubility Measurement

The solubility apparatus is assembled by MEMFO, and **Figure 3.2.** from Li et al. (2011) shows the graphical detail. The used apparatus for this thesis is identical to Li's apparatus, and a picture of the assembled apparatus is attached in **Appendix VI.**

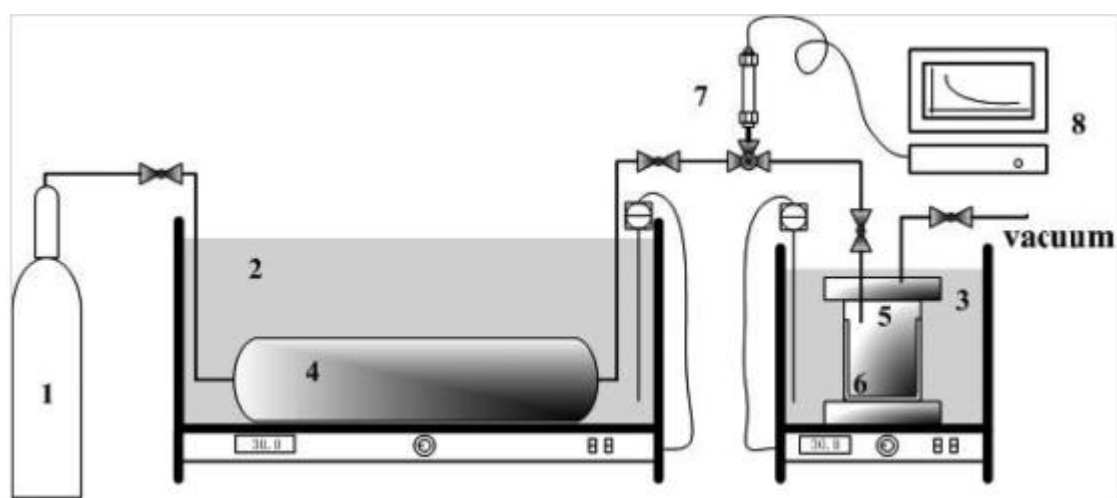


Figure 3.2. Solubility apparatus

1. Compressed CO₂ supplier, 2 & 3. Oil bath and stirrer, 4. CO₂ container, 5. CO₂ absorption vessel, 6. Cylindrical container, 7. Pressure censor, 8. Computer

The apparatus is structured by these several components: the first is the container of compressed CO₂, which is able to supply CO₂ for up to 50 bar pressure. The middle part is the gas container with a pressure censor which is able to hold CO₂ gas at a certain pressure and separated from gas supply by the first valve. Then the right one is a reaction vessel for holding the tested chemical and magnet stirrer. It is the main part for gas absorption reaction and being separated by the second valve. The whole reactor is connected to vacuum pump and the outside environment, to obtain a vacuum environment or expel the waste gas which controlled by two way valve. Both gas container and reaction vessel are in oil bath and the temperature is adjusted by a controller. A computer is connected to record the data during all processes.

Absorption:

The 5g of the sample was filled into the liquid absorption vessel. Then this vessel was connected to the gas vessel. The exhaust valve of this absorption

vessel was closed and opened the two way valve at the inlet of the gas storage vessel to vacuum side. Then vacuum pump was switched on to remove the gases from the system for about one hour. This two way valve was switched to the gas pressure side. The temperature was set to desired value and magnetic stirrer was turned on to a speed of 450 rpm. The gas vessel was filled to a desired pressure and waited for temperature and pressure to be stabilized. The middle valve between gas vessel and absorption vessel should remain closed while filling the gas into the gas vessel. When pressure was stabilized in gas storage vessel, then middle valve was opened and waited for the equilibrium to be achieved. The pressure readings before opening the middle valve and after achieving the equilibrium in absorption vessel are noted down. Then material balance gives the value of the CO₂ gas being absorbed. The aspen program was used to calculate the molar concentrations by using pressure, temperature and volume of the respective vessels.

Desorption :

The desorption process is almost in a opposite way that absorption does. Most of the settings and parameters are unchanged, but after the absorption experiment is finished, close all the valves but link the gas transmission line to the vacuum, then carefully control the first valve to make the gas container gets a pressure drop to desired pressure. Wait for about half an hour to get stabilized pressure and record, then open the second valve to connect gas container and reaction vessel, record the pressure figure again after it is stabilized. Repeat those steps until enough sets of data is recorded, aspen program will also be used in this step.

3.5. Simulation and Calculation of CO₂ Solubility

From Section 3.4., the gas pressure P_g and equilibrium pressure P_e is recorded. Referencing Redlich-Kwong Equation of State (Redlich & Kwong, 1948), the definition is:

$$P = \frac{RT}{v-b} - \frac{a}{\sqrt{T} \cdot v(v+b)}$$

In which P is pressure, V is volume, n is amount of substance, R is gas constant and T is temperature, also a and b are constants, representing by temperature and pressure of the gas in critical point (T_c and P_c), which can be set as below (Murdock, 1993, pp.25-27):

$$a = \frac{0.4275R^2T_c^{2.5}}{P_c}$$

$$b = \frac{0.08664RT_c}{P_c}$$

Since V, R, a, b are all fixed, after getting P and V could easily calculate n. The calculation is mainly done by programming of Aspen Plus V8.2.

The main screen of the simulation program is shown in the below **Figure 3.3.** and the rest detail can be found in **Appendix VII.** and **Appendix IX.**

The screenshot displays the 'Specifications' panel of the Aspen Plus V8.2 software. It is divided into several sections:

- Flash Type:** Set to 'Temperature' and 'Pressure'.
- State variables:**
 - Temperature: 140, Unit: C
 - Pressure: 1308, Unit: kPa
 - Vapor fraction: (empty)
 - Total flow basis: Volume
 - Total flow rate: 108.706, Unit: l/hr
 - Solvent: (empty)
- Composition:** Set to 'Mass-Frac'. A table below shows:

Component	Value
1	1

 Total: 1
- Reference Temperature** (collapsed)
- Component Attributes** (collapsed)
- Particle Size Distribution** (collapsed)

Figure 3.3. Main screen of CO₂ calculation, by Aspen Plus V8.2

After the input of P_g and P_e, it is possible to calculate the corresponding n_g and n_e.

After calculating the number of moles of CO₂ absorption, it is possible to find out the molar fraction of solubility x, by this following equation:

$$x_{CO_2} = \frac{n_g}{n_g + n_{solvent}}$$

After getting x, it will be plotted with P_e as a function, for better visualization and further analysis, those results will all shown in Section 4.4.

3.6. Calculation of Henry's Constant

Henry's constant (H_e) is a term that from Henry's Law (Dewulf et al., 1995), it could be presented as the following (Gui et al., 2010):

$$H_e = \lim_{x_{CO_2} \rightarrow 0} \frac{f_{CO_2}^L}{x_{CO_2}}$$
$$\approx \frac{P_e}{x_{CO_2}}$$

Among them, x is the molar fraction of solubility as discussed, and f^L is the fugacity of CO_2 . This is substituted by a following approximation.

Another methods of measuring Henry's constant is by molality H_{e_b} could be defined as follow (Li et al., 2011):

$$H_e = \lim_{x_{CO_2} \rightarrow 0} \frac{f_{CO_2}^L}{m_{CO_2}}$$
$$\approx \frac{P_e}{m_{CO_2}}$$

The **Table 3.2.** shows various Henry's constant as an example (Anthony et al., 2005), as analysis by Li (2014, pp.15), a smaller Henry's constant indicates a larger solubility. For instance, the table from Anthony et al. (2005) selects the ionic liquid 1-butyl-3-methylimidazolium hexafluorophosphate ($bmimPF_6$) as an example, it has a relatively low Henry's constant to carbon dioxide, implying a strong CO_2 solubility to other solvents in the table. Also, the Henry's constants of other gases in $bmimPF_6$ are generally far greater than CO_2 's one, while other solvents is not obvious in this aspect, this indicates $bmimPF_6$ has a great selectivity of CO_2 .

Table 3.2. Henry's constants (bar) for gases in various organic compounds (Anthony et al., 2005)

	[bmim][PF ₆]	heptane ²⁸	cyclohexane ²⁸	benzene ²⁸	ethanol ²⁸	acetone ²⁸
H ₂ O ¹³	0.17		97 ³³	10 ³³	0.1 ³⁴	0.3 ³⁴
CO ₂	53.4	84.3	133.3	104.1	159.2	54.7
C ₂ H ₄	173	44.2 ^a		82.2	166.0	92.9
C ₂ H ₆	355	31.7	43.0	68.1	148.2	105.2
CH ₄	1690	293.4	309.4	487.8	791.6	552.2
O ₂	8000	467.8	811.9	1241.0	1734.7	1208.7
Ar	8000	407.4	684.6	1149.5	1626.1	1117.5
CO	nondetect (>20 000)	587.7	1022.5	1516.8	2092.2	1312.7
N ₂	nondetect (>20 000)	748.3	1331.5	2271.4	2820.1	1878.1
H ₂	nondetect (>1500)	1477.3	2446.3	3927.3	4902.0	3382.0

^a For ethylene in hexane, not heptane.

4. Results and Analysis

4.1. P_{4444} Gly Synthesis

The resulting IR scan of synthesized P_{4444} Gly from NMR is shown below in **Figure 4.1**.

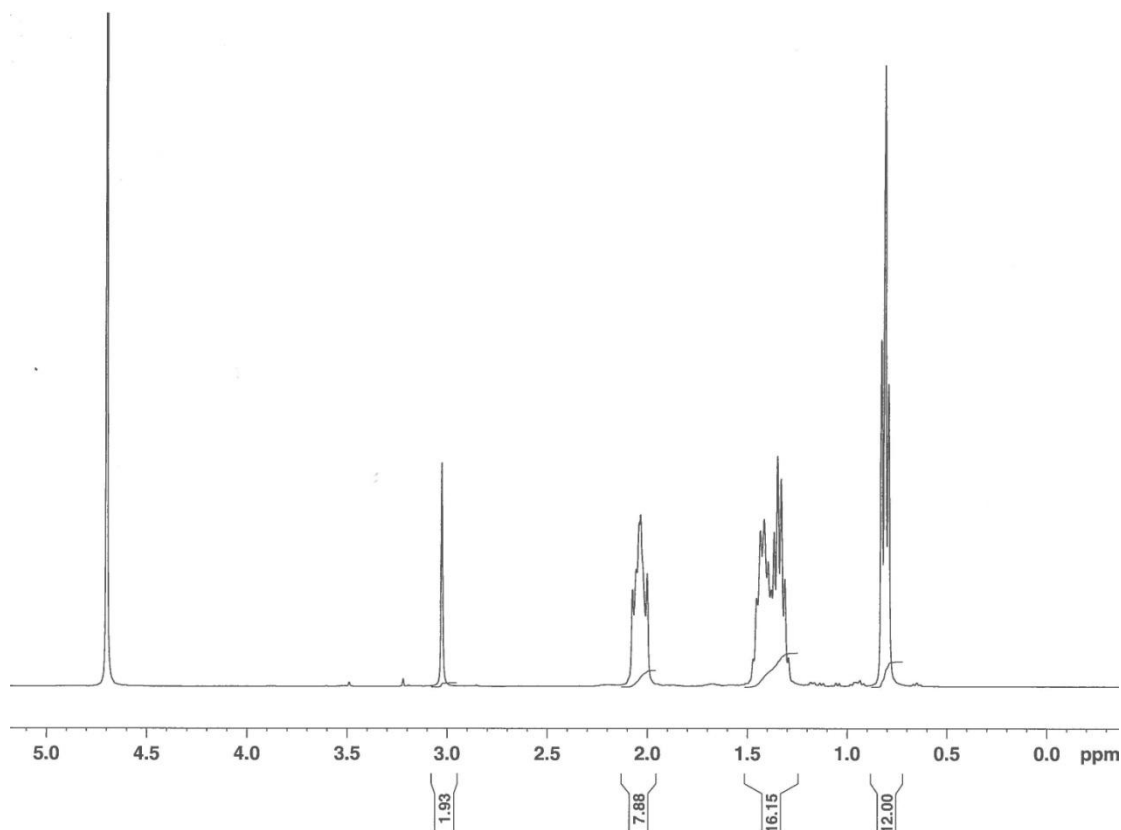


Figure 4.1. IR spectrum of P_{4444} Gly from NMR

The figure on the x-axis states the chemical displacement (δ), y-axis states the strength of targeted chemical group, in this case the proton scan gives the value of proton distribution.

From right to left, with adjusting the first peak as 12, and ignore the last peak representing D₂O. According to Zhang et al. (2006), the first δ (chemical displacement) is about 0.92 ppm, representing CH₃ with 12 protons and the second δ at about 1.34-1.52 ppm represents (CH₂)₂ with 16 protons. The third δ at 2.13-2.23 ppm stands for P-CH₂ which should own 8 protons. The last δ at 2.64 ppm is the functional group of N-CH₂-CO₂, which is supposed to be 2 protons.

By the comparison of adjusting result and literature, the figure clearly shows 4 peaks with similar δ values at x-axis as reported by Zhang et. al. (2006). This indicates that the P₄₄₄₄Gly product is very pure and it is in strong agreement with the literature data. In addition, there are also two small hetero peaks in the scan but those are insignificant. As lot of amount of ionic liquid was required to run the experimental measurements, different batches of ionic liquid P₄₄₄₄Gly were synthesized and purity was tested with NMR scans. Rests of the scans are attached in *Appendix VIII*.

4.2. Density Measurements

The density measurements are run for both pure PEG400 and P₄₄₄₄Gly and their blends (0.70P₄₄₄₄Gly-0.30PEG400, 0.5P₄₄₄₄Gly-0.5PEG400, 0.3P₄₄₄₄Gly-0.7PEG400) in a temperature range of 20 °C to 80 °C.

The results obtained from density measurements are plotted in the following **Figure 4.2**. And the original table from density measurements is tabulated in **Appendix X**.

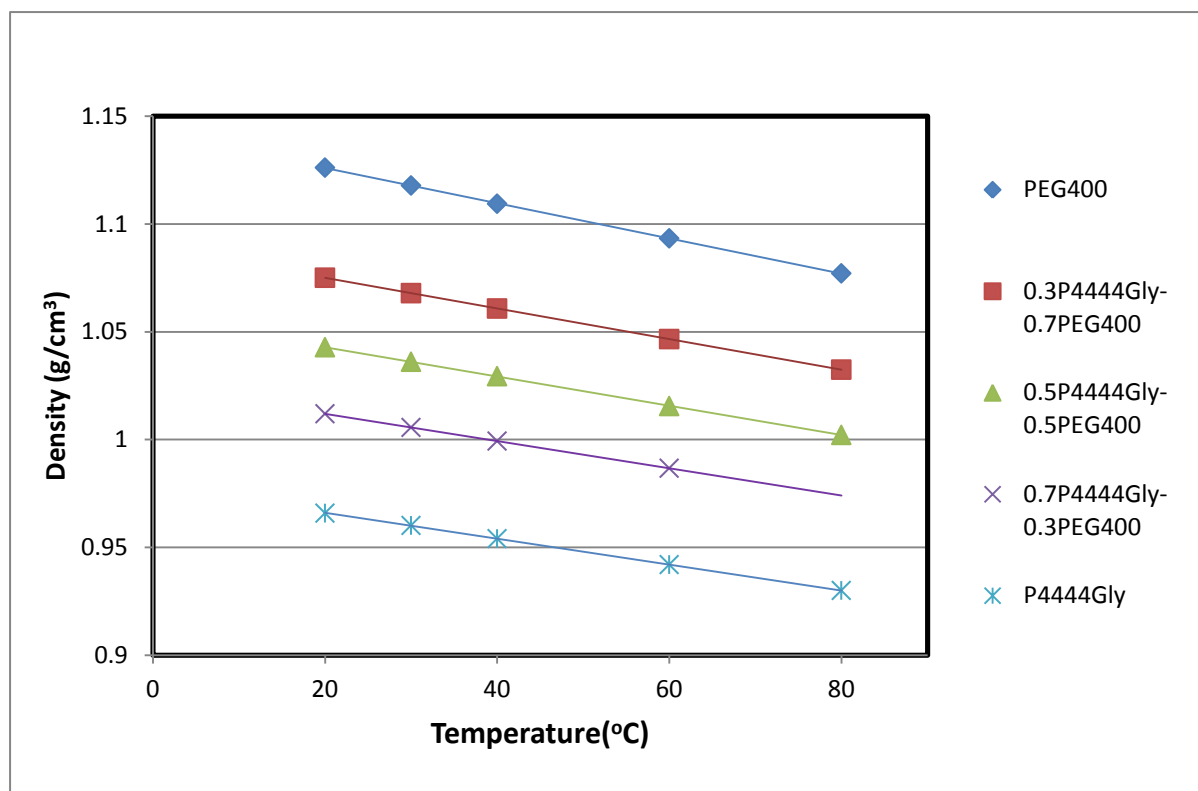


Figure 4.2. Density of P₄₄₄₄Gly, PEG400 and their blends

The density results clearly predicts that density of all the samples decreases with the increase in temperature. The density of PEG400 is the highest and that of P₄₄₄₄Gly is the least. As concentration of P₄₄₄₄Gly is increased, the density of the blend also decreased.

For the accuracy of experimental measurements, de-ionised water was also run and data were compared with literature. However, as ionic liquid used in this study is new and literature data is not available for the comparison but density data for PEG400 is available. Select this work with the result from Han et al. (2008). Trivedi et al. (2010). Eliassi et al. (1998). Wu et al. (2010) then plotted in **Figure 4.3**. The original table for numeral data is in

Appendix XI. From the graph in *Figure 4.3.*, the results look quite in agreement with the already reported data.

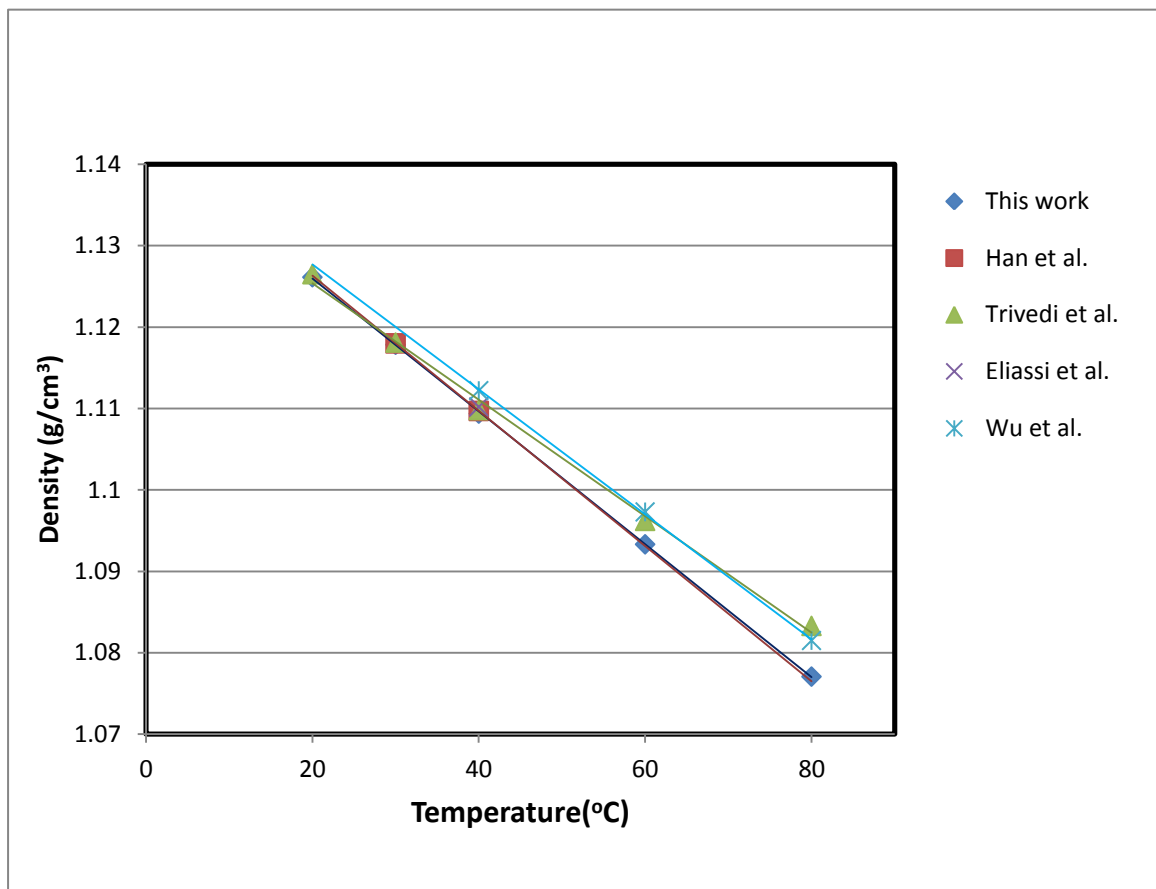


Figure 4.3. Comparison of PEG400 density

The % error is in the range of 0.0143-0.364% which indicates that our measurements are accurate and within the acceptable error range.

However, the difference between this work and Wu et al. (2010), Trivedi et al. (2010) is relatively big. This is due to the Wu's measuring temperature is not accurate, and probably Trivedi's chemical does not reach analytical purity, according to the given producer's detail.

Temperature range for absorption experiments selected is 60-140 °C but the maximum operating temperature of our apparatus is 80 °C. Therefore, data from density measurements is extrapolated to 140 °C by fitting the data to linear trend line.

The equation parameters are reported in *Table 4.1.*

Table 4.1. Linear approximation of density graph

Component	Equation
P₄₄₄₄Gly	$\rho = -0.0006T + 0.978$
0.7P₄₄₄₄Gly-0.3PEG400	$\rho = -0.0006T + 1.0246$
0.5P₄₄₄₄Gly-0.5PEG400	$\rho = -0.0007T + 1.0565$
0.3P₄₄₄₄Gly-0.7PEG400	$\rho = -0.0007T + 1.0892$
PEG400	$\rho = -0.0008T + 1.1423$

For future use of density approximation in 100, 120 and 140 °C, *Table 4.2.* provides necessary density data by this equation.

Table 4.2. Approximated density data in higher temperature

Component	Density (g/cm ³)		
	100 °C	120 °C	140 °C
P₄₄₄₄Gly	0.918	0.906	0.894
0.7P₄₄₄₄Gly-0.3PEG400	0.9646	0.9526	0.9406
0.5P₄₄₄₄Gly-0.5PEG400	0.9865	0.9725	0.9585
0.3P₄₄₄₄Gly-0.7PEG400	1.0192	1.0052	0.9912
PEG400	1.0623	1.0463	1.0303

In the solubility part (Chapter 4.) the density data will be directly used in the calculating excel sheet.

4.3. Viscosity Measurement

In this section, sample of pure PEG400 and 0.3P₄₄₄₄Gly-0.7PEG400 are measured at 25-120 °C. The results of viscosity measurements are shown in **Figure 4.3.**, and the original data is tidied as table and attached in **Appendix XII.**

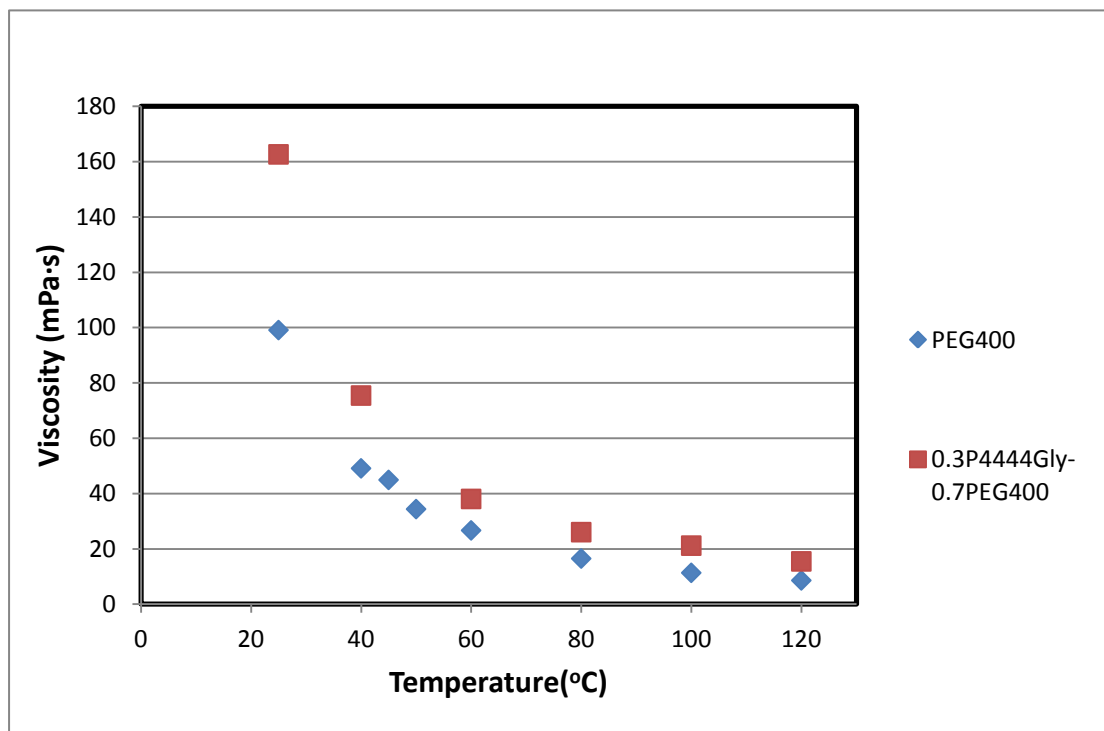


Figure 4.3. Viscosity data of PEG400 and 0.3P₄₄₄₄Gly-0.7PEG400

As the figure shows, the viscosity of both PEG400 and mixture of 0.3P₄₄₄₄Gly-0.7PEG400 decreases when temperature increases. Among them, the decreasing speed of 0.3P₄₄₄₄Gly-0.7PEG400 is much higher than the speed of PEG400.

The data for ionic liquid is scarcely available in the literature but viscosity of PEG400 is investigated by different authors: Jerome et al. (1968). Han et al. (2008)., Gourgouillon et al. (1998)., Ottani et al. (2012). Wu et al. (2010), the resulting figure is easily set up and shown in **Figure 4.4.**, the original data from **Appendix XIII.**

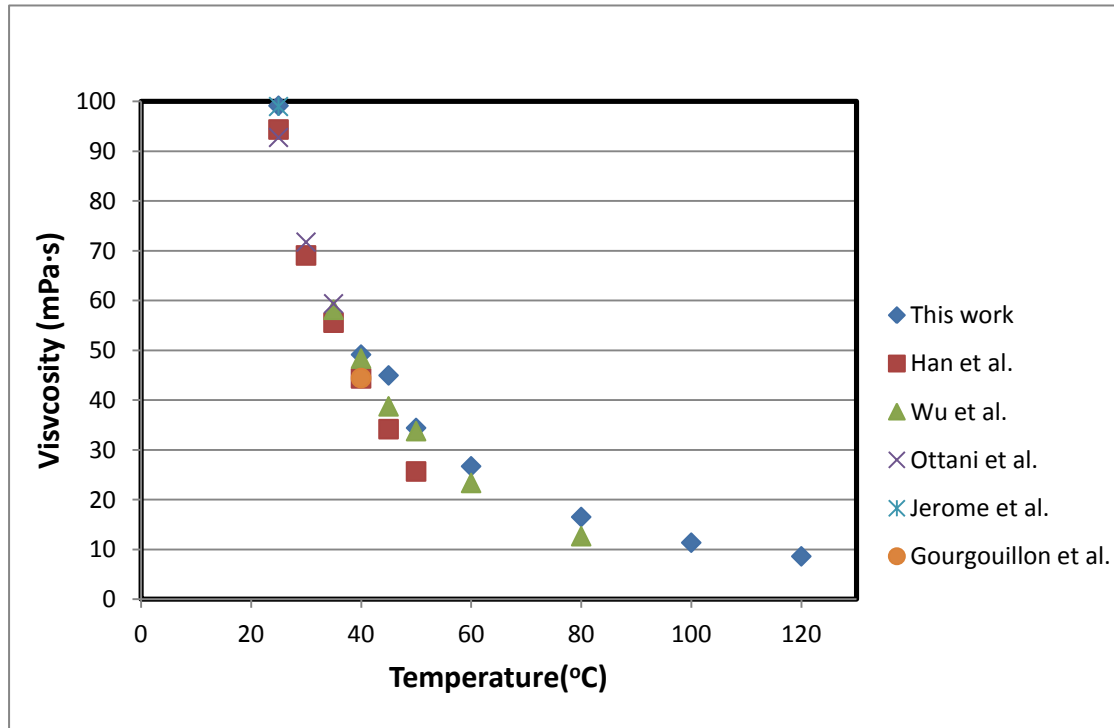


Figure 4.4. Comparison of PEG400 viscosity

It is observed that, the data of this work has error with a range from 0.162-34.05% corresponding to the literature values. And surprisingly, all literature values have large error with each other from 0.135-31.56%. It is not easy to predict the accuracy of the data. The rheometer that has been used for the viscosity studies is recently purchased and under development for experimental procedures. That is why large error is reported if one particular literature is compared. In order to confirm the accuracy, another experiment of standard viscosity solution following a similar procedure was designed.

The result of experiment and the reference data from manufacturer is on **Table 4.3.**, and a graph for visualization is provided in **Appendix XIV.**

Table 4.3. Viscosity comparison of standard viscosity solution for rheometer used and reference value from manufacturer

Temperature	Viscosity (mPa s)		
	This work	Reference from Producer	% Error
25 °C	588.3	573.8	2.53%
40 °C	189.7	182.6	3.89%
50 °C	99.66	94.07	5.94%
60 °C	59.87	51.95	7.92%

80 °C	22.59	19.02	18.77%
100 °C	10.29	8.465	21.56%

Based on the error calculation, it comes to the conclusion that, results from this rheometer gives large error up to 21% as rising the temperature. The error is acceptable in low temperature, e.g. 2.53% in 25 °C, but then it becomes larger during increasing of temperature, until 21.56% in 100 °C. The result in lower temperature might be used, but not the higher temperature.

As procedures for Rheometer is under development phase for ionic liquids and blends, therefore, these results could be used as an estimation of viscosity effect on CO₂ solubility, it also gives the idea of the rough viscosity range, as well as viscosity change of ionic liquid with the addition of PEG400.

4.4. CO₂ Absorption and Desorption by Chemical

4.4.1. Absorption and Desorption of Pure PEG400

For pure PEG400, the result of CO₂ absorption and desorption in 40, 60, 100 and 140 °C are shown in **Figure 4.5**. below.

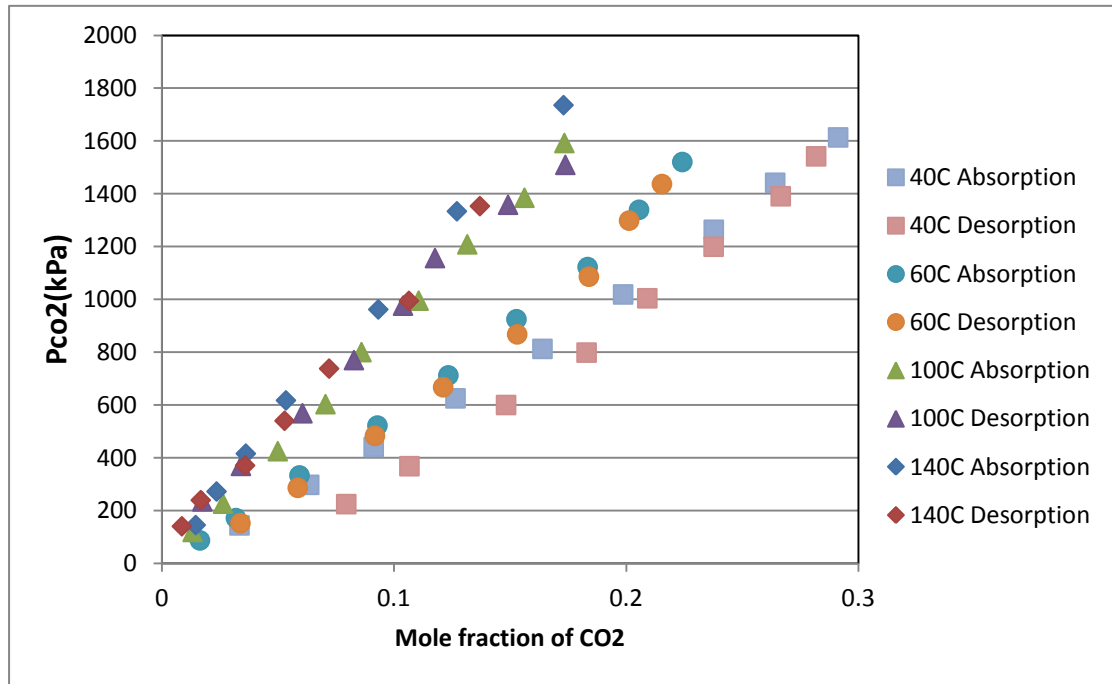


Figure 4.5. CO₂ absorption and desorption of PEG400

The figure shows that, the absorption and desorption of PEG400 has an approximate linear relationship of CO₂ amount versus pressure, and the absorption and desorption line are close to each other. This confirms that, the mechanism of CO₂ capture by PEG400 is a physical absorption, the process is reversible when the solvent is desorbing with reduced pressure.

Another result is, the CO₂ solubility in PEG400 is relatively good compared to most physical solvent, which agrees the result from literature. Similar as other solvents, the PEG400 solubility has an inverse proportion versus temperature, but it only decreases slightly when temperature increases in the interval of 100 °C to 140 °C.

Comparisons between this work and Li et al. (2011) in 40 °C and 60 °C are also provided in **Figure 4.6**. Also another attachment of original literature data is provided in **Appendix XV**.

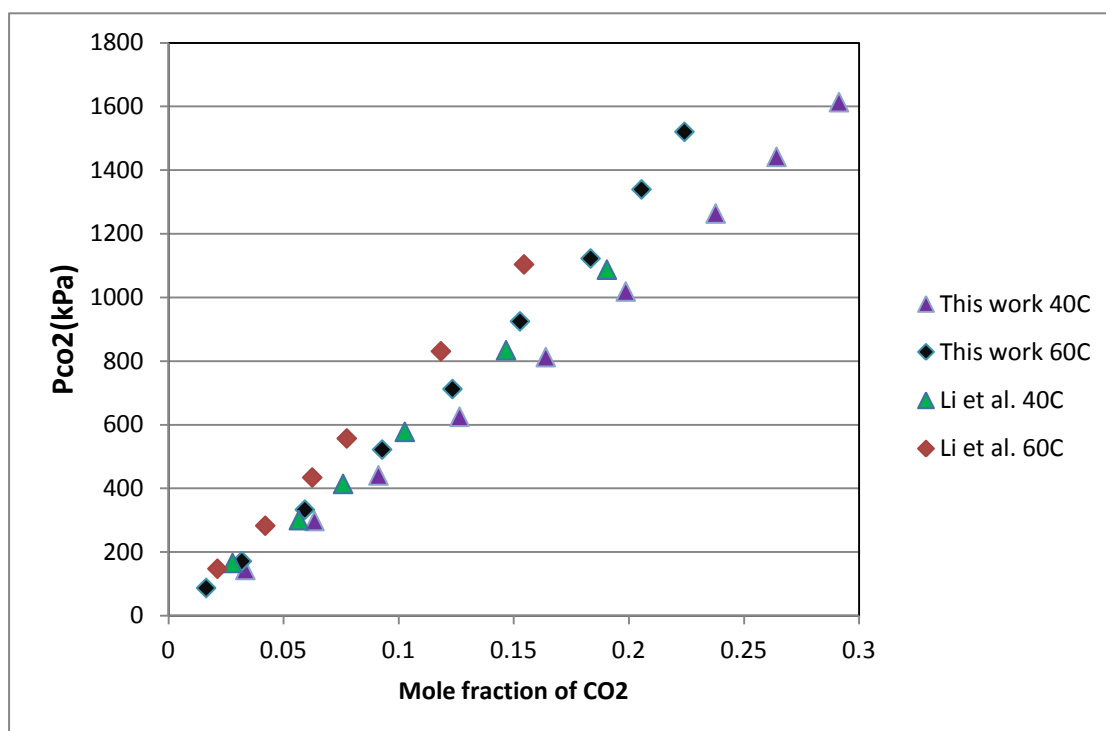


Figure 4.6. CO₂ absorption of PEG400 compare with literature data

From the comparison, it is possible to conclude that experimental data agrees very well with the literature data within an accuracy of 3%. In order to confirm the credibility of this work, another comparison will be shown in Section 4.4.3., and repeated experiments for more accuracy is strongly recommended.

Since the absorption and desorption of the PEG400 is identical at approximately all the temperatures, however, it is observed that PEG400 solution changed colour after experiment at 140 °C, as what **Figure 4.7.** shows. Which implies that PEG400 might decompose during high temperature, and thus a lower temperature is recommended to reduce this effect.

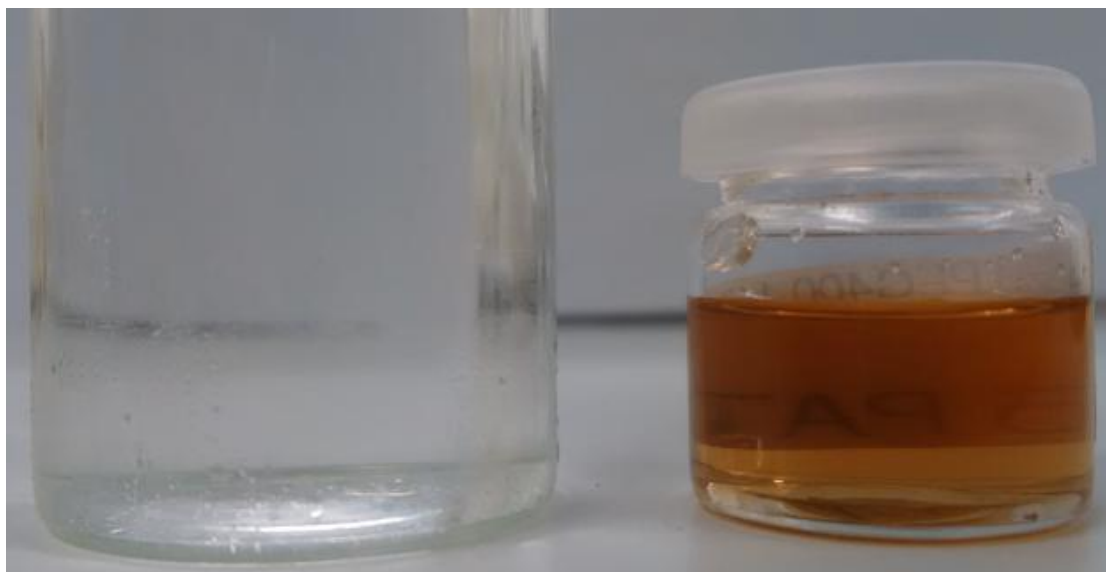


Figure 4.7. Comparison of PEG400 before experiment (left) and after the experiment (right) at 140 °C

4.4.2. Absorption and Desorption of Pure P₄₄₄₄Gly

For pure P₄₄₄₄Gly, only experiments of absorption and desorption up to 18 bar at 60 °C and 100 °C are done due to the time limitation, the result of CO₂ absorption and desorption are shown in **Figure 4.8.** below.

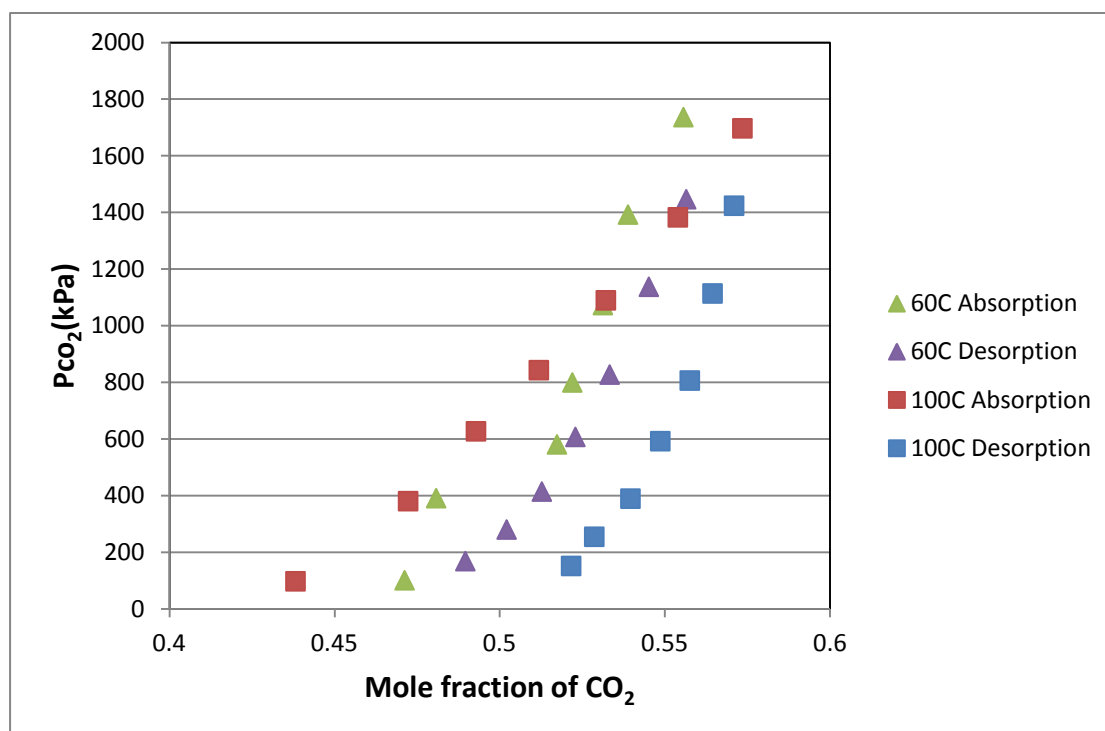


Figure 4.8. CO₂ absorption and desorption of P₄₄₄₄Gly

Unlike the result graph of PEG400, the CO₂ solubility of P₄₄₄₄Gly is clearly non-linear, this obeys the previous conclusion from literature that P₄₄₄₄Gly is chemical absorption mainly. And CO₂ solubility decreases obviously when increasing temperature, which also state that this chemical absorption corresponds to the general regular of gas solubility.

One special phenomenon is worth considering: for P₄₄₄₄Gly absorption in low temperature and low pressure, it usually takes very long time for fully stabilization of equilibrium pressure. This is probably due to high viscosity of the ionic liquid, which negatively affects CO₂ absorption.

The screenshot below is one of the example. This case took more than 8 hours for stable equilibrium pressure to be achieved, and the pressure has dropped down for approximately 20kPa. This issue is similar to what Hasib-ur-Rahman et al.'s research (2010) presents. Screenshot of this issue is in **Figure 4.9.**

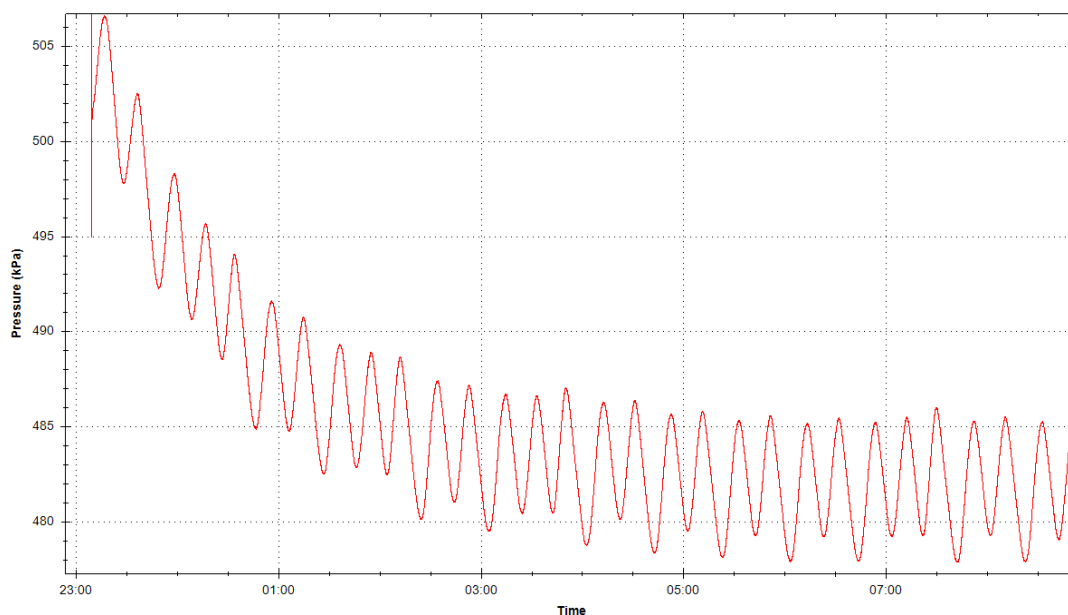


Figure 4.9. Screenshot of P₄₄₄₄Gly absorption in low pressure

The direct application of pure P₄₄₄₄Gly is not recommended and the **Figure 4.10. below** explains the reason.

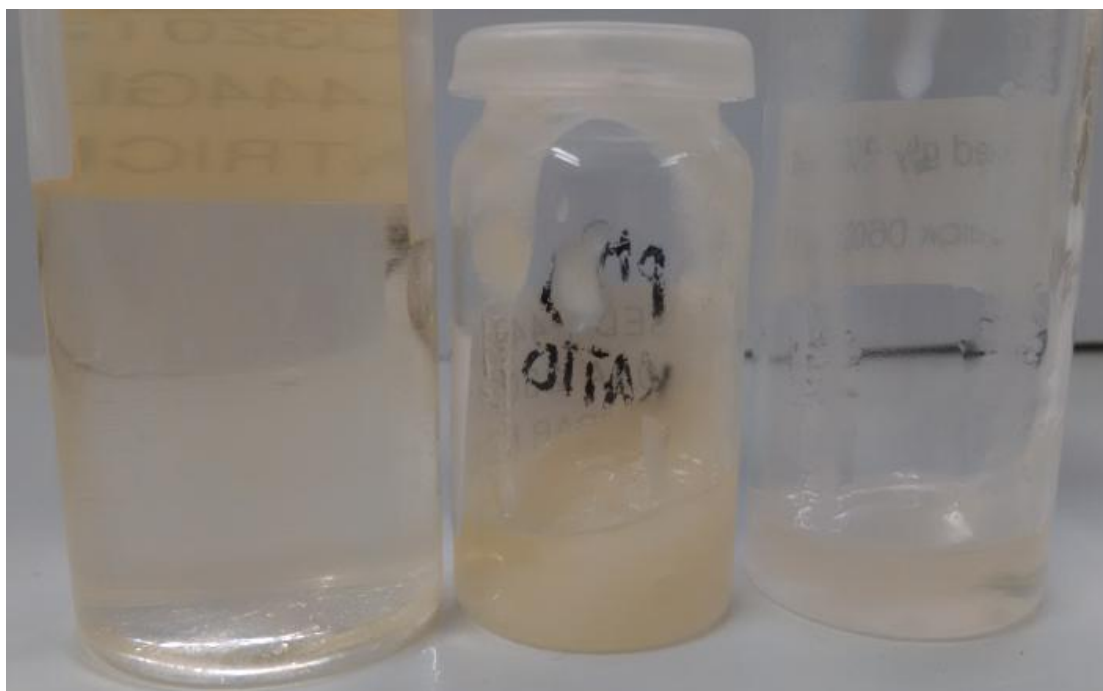


Figure 4.10. Comparison of P₄₄₄₄Gly before experiment, after 60 °C absorption and after 100 °C absorption (from left to right)

It is clearly seen that, the CO₂ solubility of P₄₄₄₄Gly is with good effects, but

the sample is solidified after absorption at 60 °C. Comparatively, the sample after 100 °C is not solidified, but still became highly viscous with a glue-like texture. As a summary, this agrees with the literature review in Chapter 2, adding PEG400 as diluting agent is necessary and potentially helpful. It is also the basis of the next several experiments.

4.4.3. Absorption and Desorption of 0.3P₄₄₄₄Gly-0.7PEG400

For further study, the ionic liquid P4444Gly was blended with PEG400 in order to overcome the problem of viscosity and absorption-desorption tests were run for different concentrations of PEG400 and P4444Gly. From these results, we can optimize the concentration of ionic liquid for CO₂ solubility. For 0.3P₄₄₄₄Gly-0.7PEG400, the result of CO₂ absorption and desorption are presented in **Figure 4.11**. below.

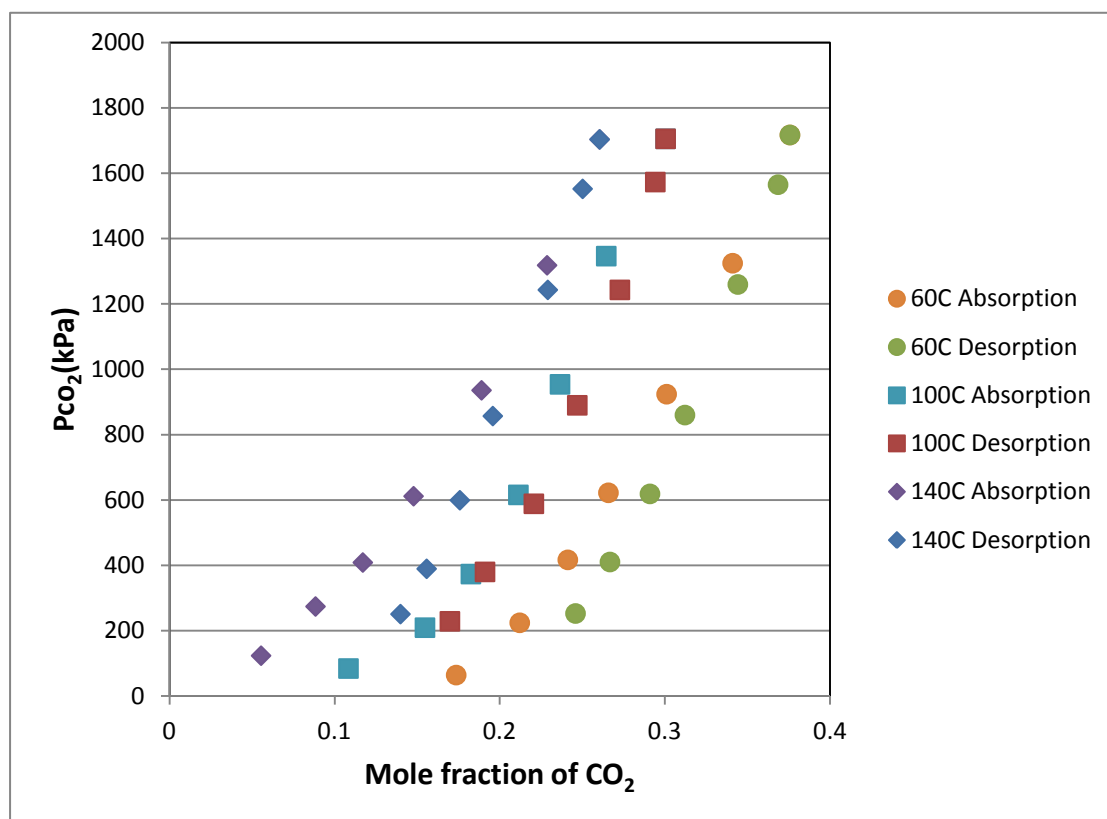


Figure 4.11. CO₂ absorption and desorption of 0.3P₄₄₄₄Gly-0.7PEG400

The results clearly show that CO₂ solubility is reduced with increasing the temperature and more gas will be absorbed at high pressure due to large driving force available.

With analyzing the above data, the strong non-linearity shows that the mixture is still dominated by chemical absorption. On the other hand, when mixing with PEG400, the system has reduced viscosity, and results in spending less time to reach equilibrium. In this case, diffusivity of CO₂ in ionic liquid is higher due to less viscosity and hence the solubility, the addition of PEG400 gets a positive effect on absorbing CO₂ more efficiently.

The absorption data is compared with the literature data (Li, 2014), and the result is shown in *Figure 4.12*.

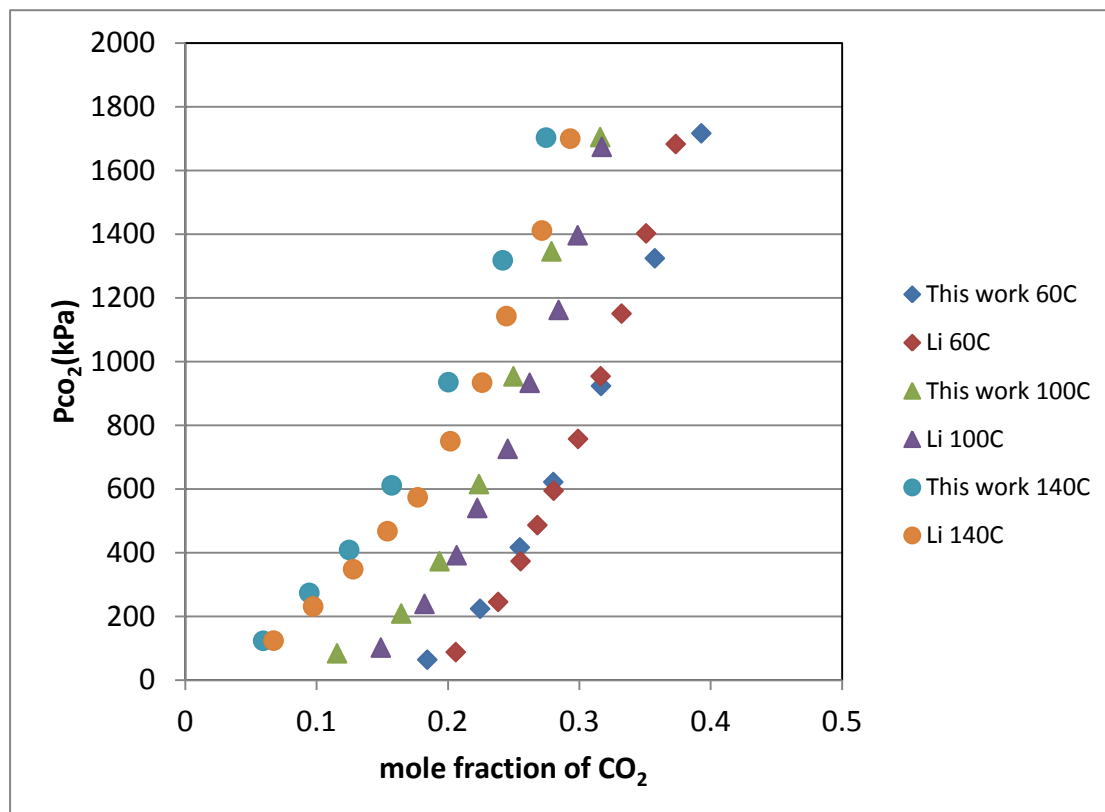


Figure 4.12. CO₂ absorption of 0.3P₄₄₄₄Gly-0.7PEG400 compare with literature data

According to the above comparison, the experimental result basically fits the literature data, with a similar tendency and less overlap with other curves. The minute error in the measurements could be the result of temperature control of the equipment which is totally based on the oil bath temperature.

Figure 4.13. shows the original mixture and the collected sample after those three experiments.



Figure 4.13. Comparison of 0.3P₄₄₄₄Gly-0.7PEG400 before experiment, after 60 °C, 100 °C and 140 °C experiment (from left to right)

Here we see again solid formation at 60 °C, but the solid formation was dramatically reduced at 100 °C, and there is almost no solid found on 140 °C sample. That also proves from another aspect that solid formation could be reduced if the sample is desorbed at 140 °C.

4.4.4. Absorption and Desorption of 0.5P₄₄₄₄Gly-0.5PEG400

For 0.5P₄₄₄₄Gly-0.5PEG400, the result of CO₂ absorption and desorption are shown in *Figure 4.14.* below.

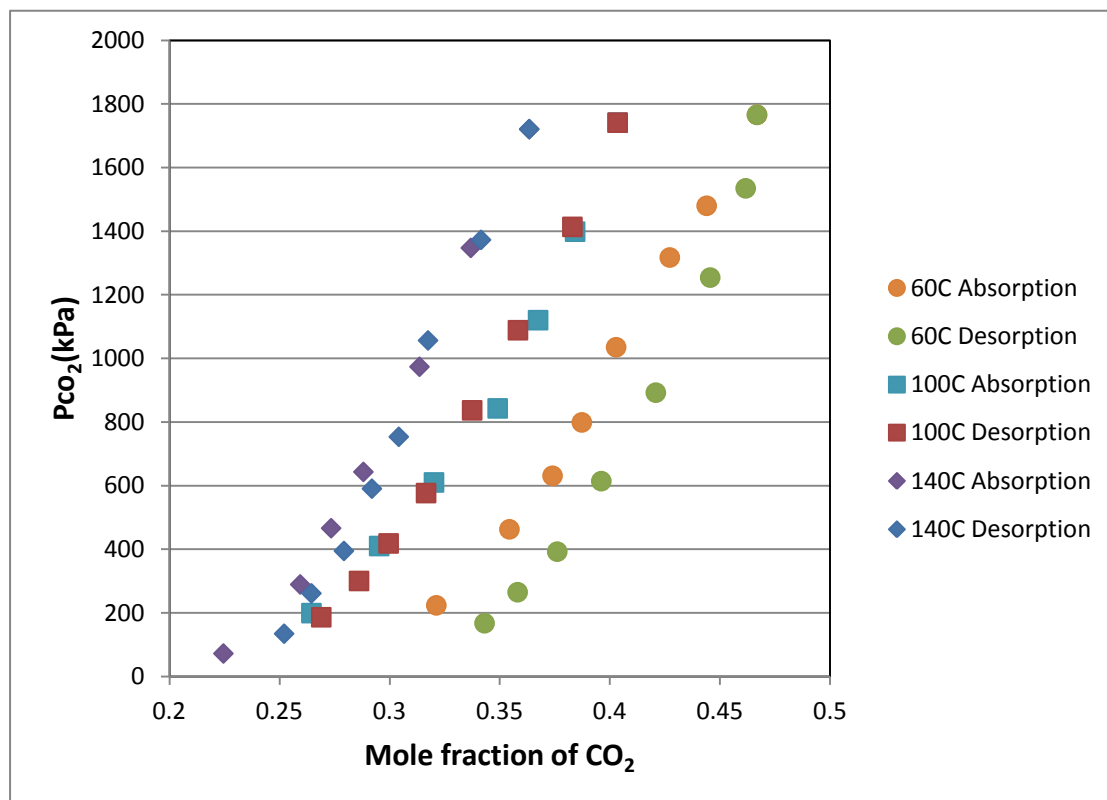


Figure 4.14. CO₂ absorption and desorption of 0.5P₄₄₄₄Gly-0.5PEG400

As well *Figure 4.15.* shows the sample solution before and after these experiments.

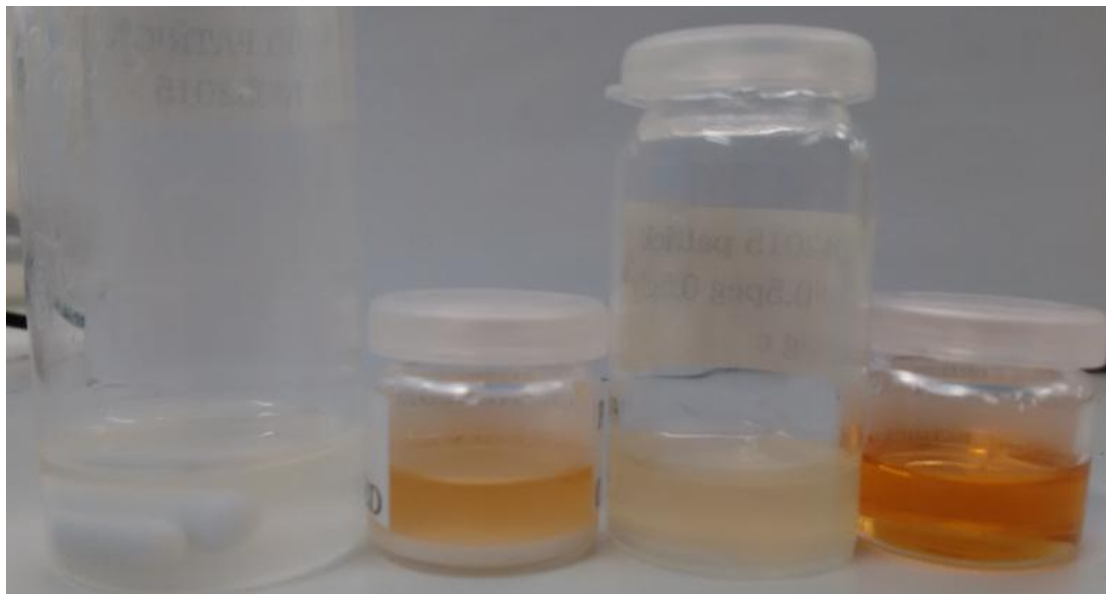


Figure 4.15. Comparison of 0.5P₄₄₄₄Gly-0.5PEG400 before experiment, after 60 °C, 100 °C and 140 °C experiment (from left to right)

(from left to right: 0.5P₄₄₄₄Gly-0.5PEG400 before experiment, after the experiment at 60 °C, 100 °C, 140 °C respectively)

As seen on figure, there is slight colour change in at both 60 °C and 100 °C sample, in which 100 °C changes a bit more. And the colour of sample is greatly deepen as dark-brown after 140 °C experiment, this leads to idea of further NMR scan and analysis, and also brings up the importance of setting a reasonable operating temperature.

4.4.5. Absorption and Desorption of 0.7P₄₄₄₄Gly-0.3PEG400

For 0.7P₄₄₄₄Gly-0.3PEG400, the result of CO₂ absorption and desorption is shown in *Figure 4.16.* below.

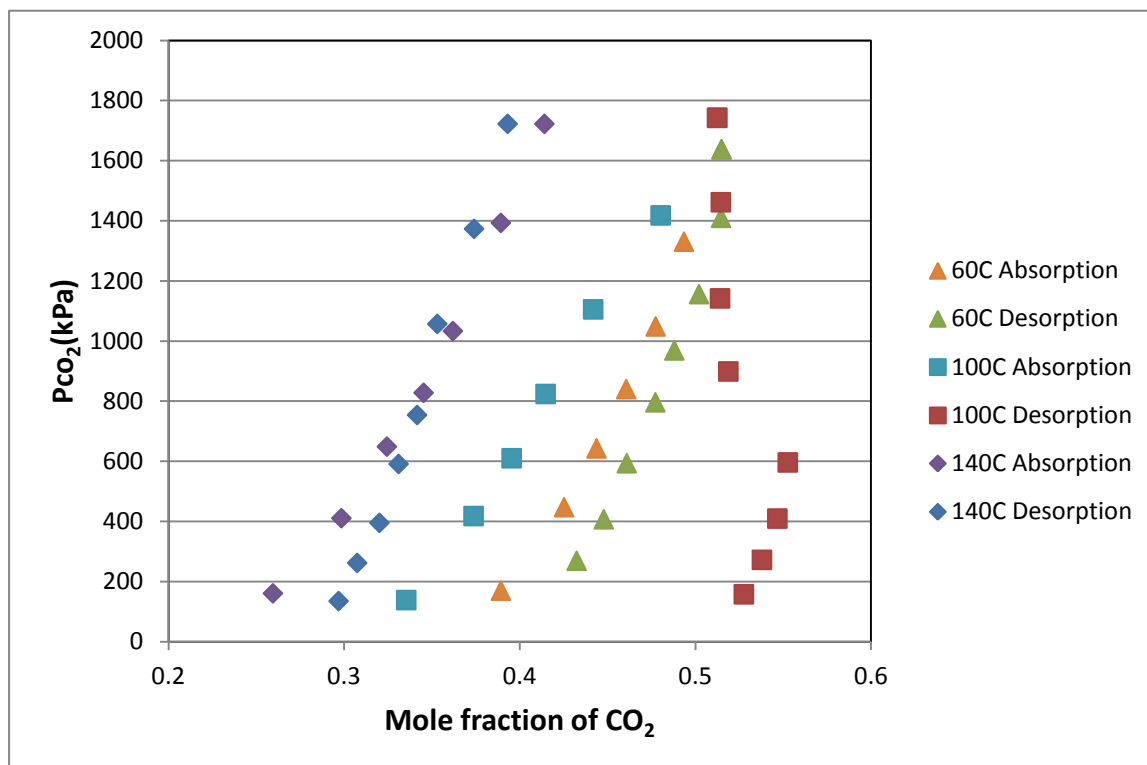


Figure 4.16. CO₂ absorption and desorption of 0.7P₄₄₄₄Gly-0.3PEG400

Among them, it is clearly seen that the data of 100 °C is clearly abnormal, currently the exact answer is not found, perhaps it is because of accidental apparatus leakage or any false operation.

As well *Figure 4.17.* is the sample solution before and after these experiments.



Figure 4.17. Comparison of 0.7P₄₄₄₄Gly-0.3PEG400 before experiment, after 60 °C, 100 °C and 140 °C experiment (from left to right)

Although there is a bit abnormal data, mostly the data is reasonable and in line with expectation. No matter which ratio, increasing temperature stimulates more absorption and decreasing temperature stimulates more desorption. Hence, for further experiment, it is recommended to adjust the absorption temperature at 60 °C and desorption temperature at 140 °C.

In order to get a more comprehensive result, the graph is sorted by temperature at the next section. Results and recommendations is given as well after the comparison.

4.5. CO₂ Absorption and Desorption by Temperature

4.5.1. Absorption and Desorption at 60 °C

To study the effect of temperature and concentration of ionic liquid on CO₂ solubility can be better viewed by plotting all the results of different concentration at a single temperature on one graph. The absorption and desorption results at 60 °C are shown in *Figure 4.18.* and *Appendix XVI.*

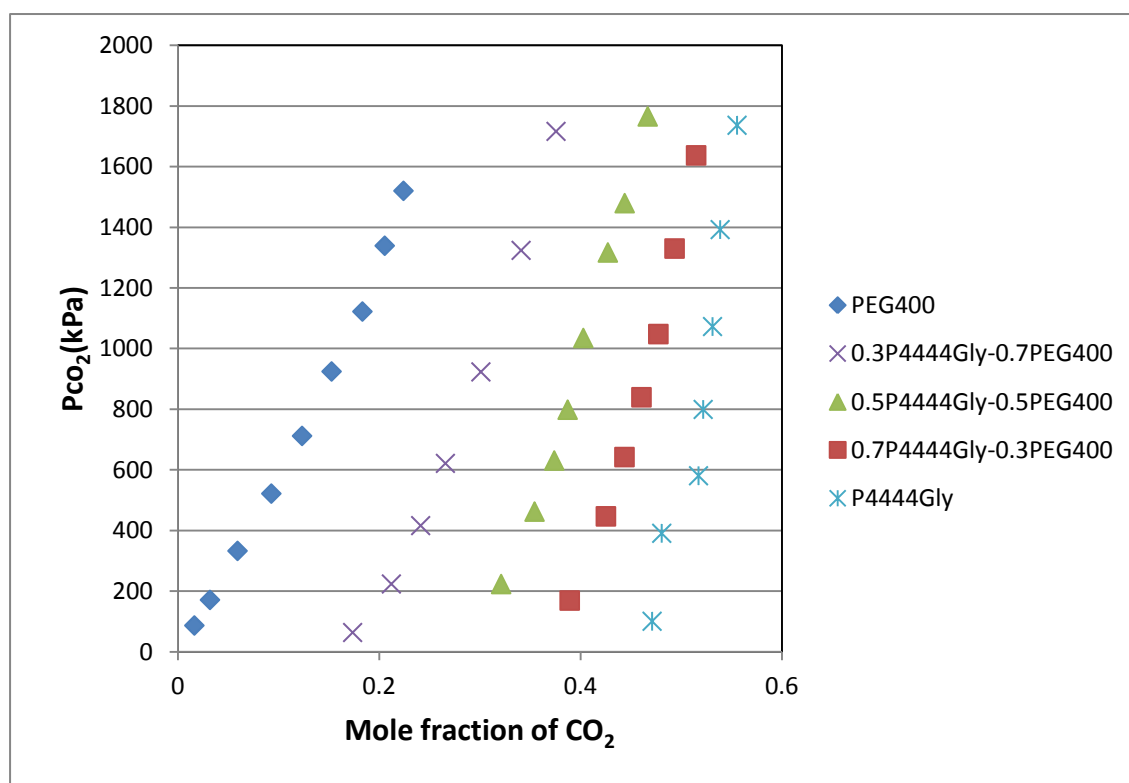


Figure 4.18. CO₂ absorption data at 60 °C

In this graph, it is clearly seen that, the absorption effect rapidly increases, then become slower after the concentration of P₄₄₄₄Gly increases. Taken together, the ratio 0.5P₄₄₄₄Gly-0.5PEG400 gets the most suitable effect.

4.5.2. Absorption and Desorption at 100 °C

Also *Figure 4.19.* and *Appendix XVII.* shows the absorption and desorption data.

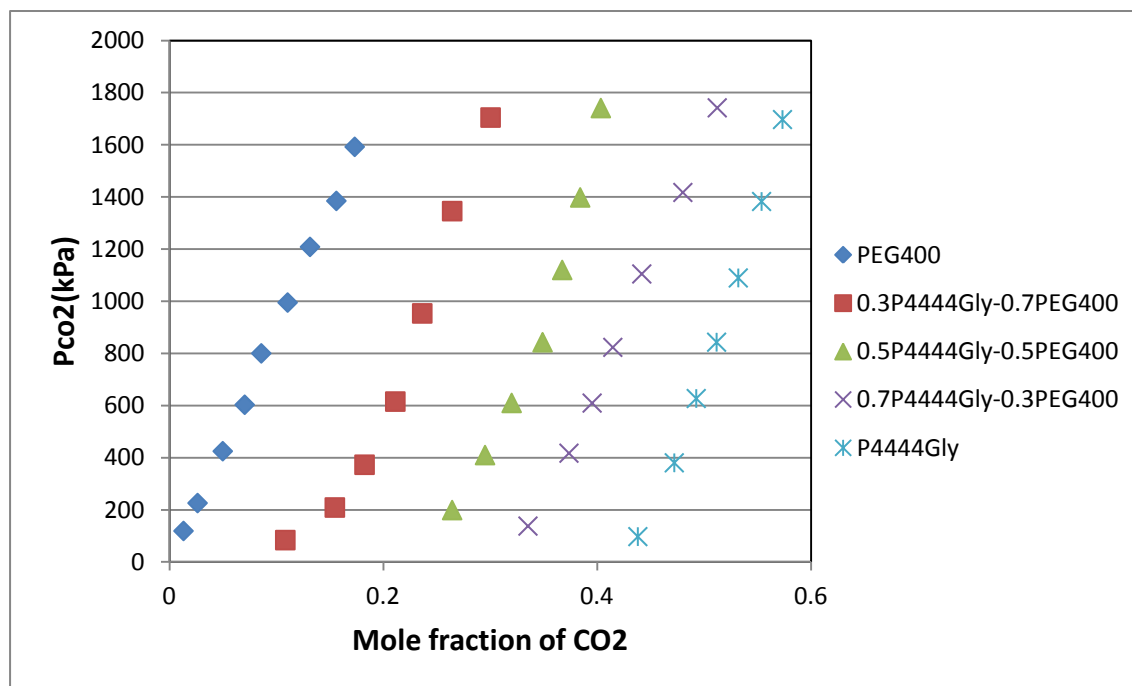


Figure 4.19. CO₂ absorption data at 100 °C

Both of them has similar results as 60 °C, except for the desorption data of 0.7P4444Gly-0.3PEG400 is abnormal. Also similar recommendations can be put forward.

4.5.3. Absorption and Desorption at 140 °C

Because of the time insufficient, the experiment of pure P4444Gly is missing, the rest of result are displayed on *Figure 4.20.* and *Appendix XVIII.*

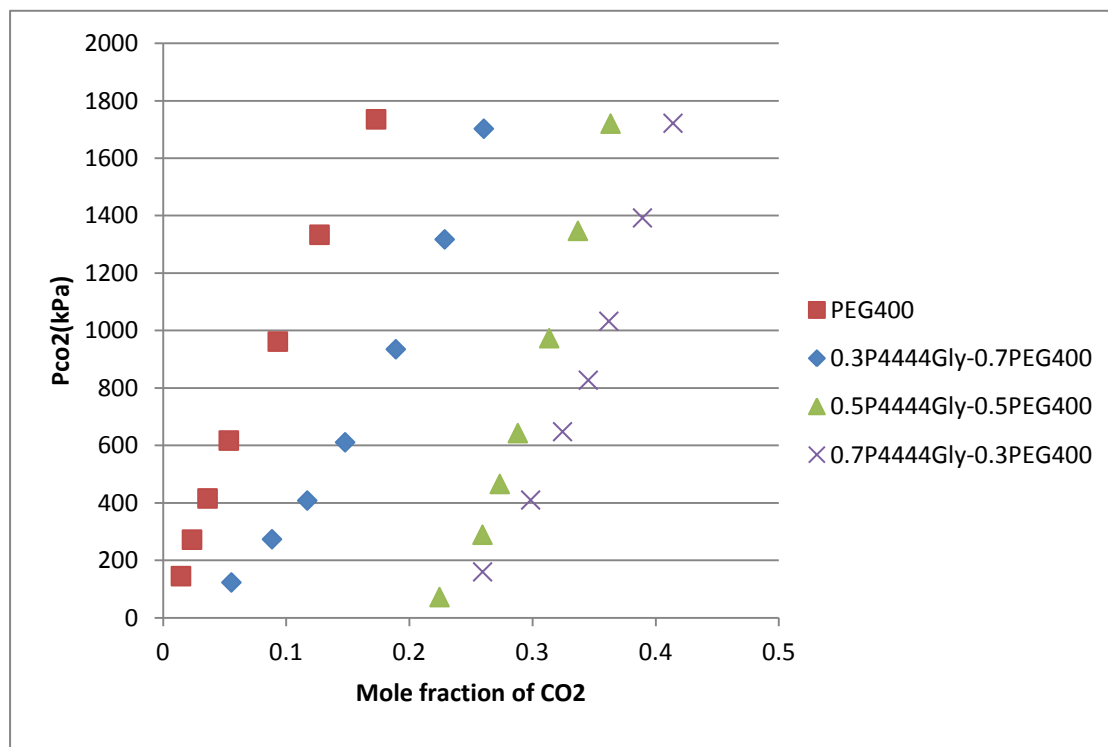


Figure 4.20. CO₂ absorption data at 140 °C

Comparing with those graphs, it is obvious that, the CO₂ solubility increases when concentration of P₄₄₄₄Gly increases, however, the increasing rate slowly reduces during this process. On the other hand, high P4444Gly content leads to high viscosity and slow reaction rate, therefore a middle point should be found. Without detailed research of the exact ratio, in current steps it is evaluated that 0.5P₄₄₄₄Gly-0.5PEG400 is the most suitable point for this experiment, due to its effect satisfies both criteria.

4.6. Result of Cyclic Capacity Experiment

The cyclic capacity of any solvent is very important for its selection as an absorbent to be employed. So, a cyclic capacity experiment was run with 0.3P₄₄₄₄Gly-0.7PEG400, with three times absorption at 60 °C and desorption at 140 °C. The result is shown in *Figure 4.21.* below.

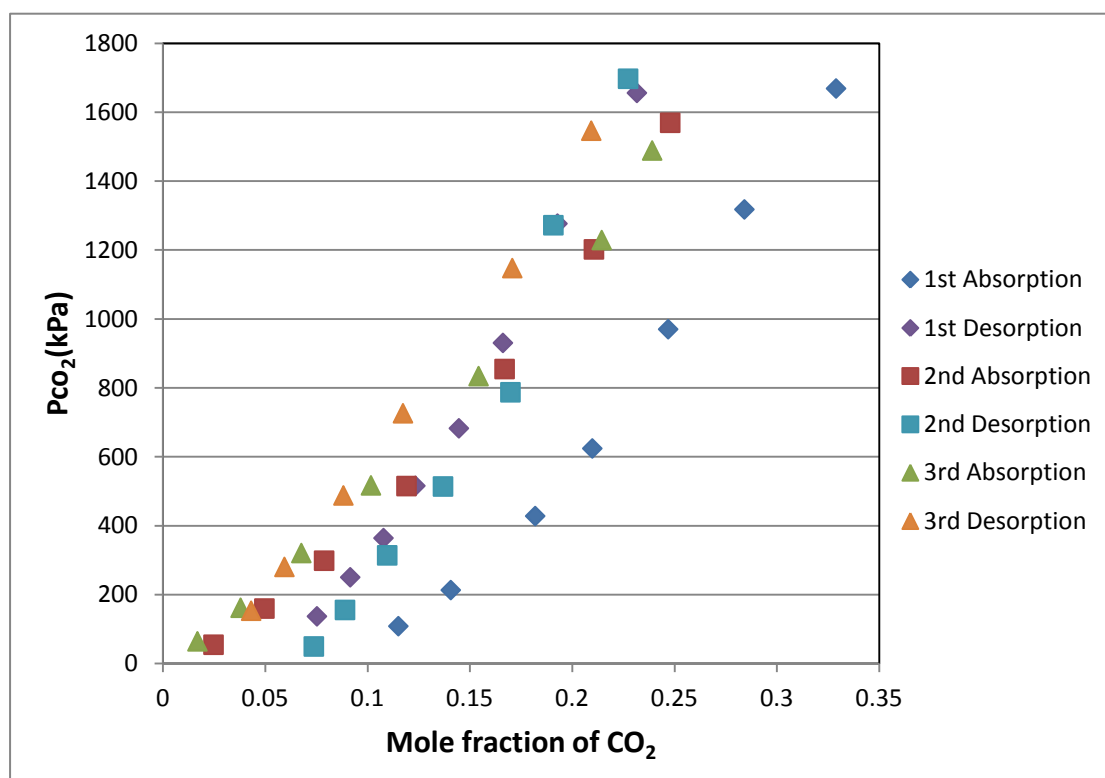


Figure 4.21. Cyclic capacity experiment of 0.3P₄₄₄₄Gly-0.7PEG400

It leads to a conclusion that, there is obvious difference between absorption and desorption at the first cycle, then the difference is almost eliminated at the second and third cycles. In other words, the absorption and desorption recurrence has a very well result at the first time, then it becomes unfavourable in the following cycle. Therefore, in the current situation, it is not very realistic for repeated use.

In addition, *Figure 4.22.* shows the 0.3P₄₄₄₄Gly-0.7PEG400 sample of 140 °C experiment and the cyclic capacity experiment.

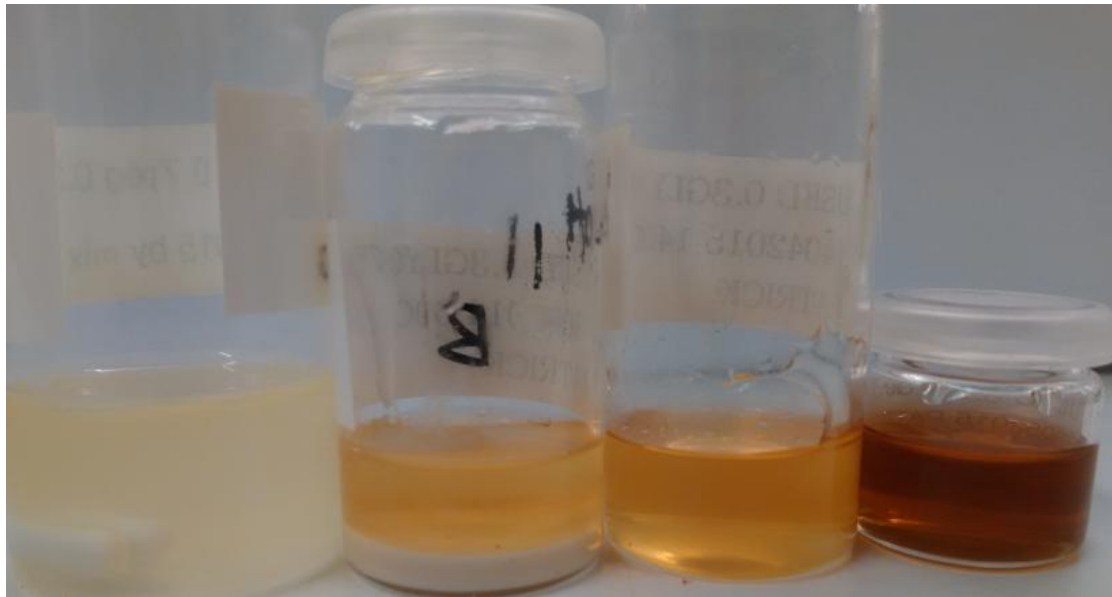


Figure 4.22. Comparison of 0.3P₄₄₄Gly-0.7PEG400 before experiment, after 60 °C, 140 °C, and cyclic capacity experiment (from left to right)

The similarity of both experiments are with the same constituent and same highest temperature, however the cyclic capacity solution has a deeper colour, Based on the fact that the processing period of cyclic capacity experiment is much longer, this colour difference and decomposition are probably due to the heating time, more advanced method of reducing heating period might applied and improve this whole process.

4.7. Improvement and Results

From the conclusion of upper sections, 100 °C is too low for complete desorption, but 140 °C might be too high and cause metamorphism, a better point might exist between these two points. Based on this thinking, this section aims to try an improving experiment at 120 °C for desorption of ionic liquid system, the 0.7P₄₄₄₄Gly-0.3PEG400 mixture is used for sample.

For 120 °C , the result of CO₂ absorption and desorption is shown in **Figure 4.23**. below.

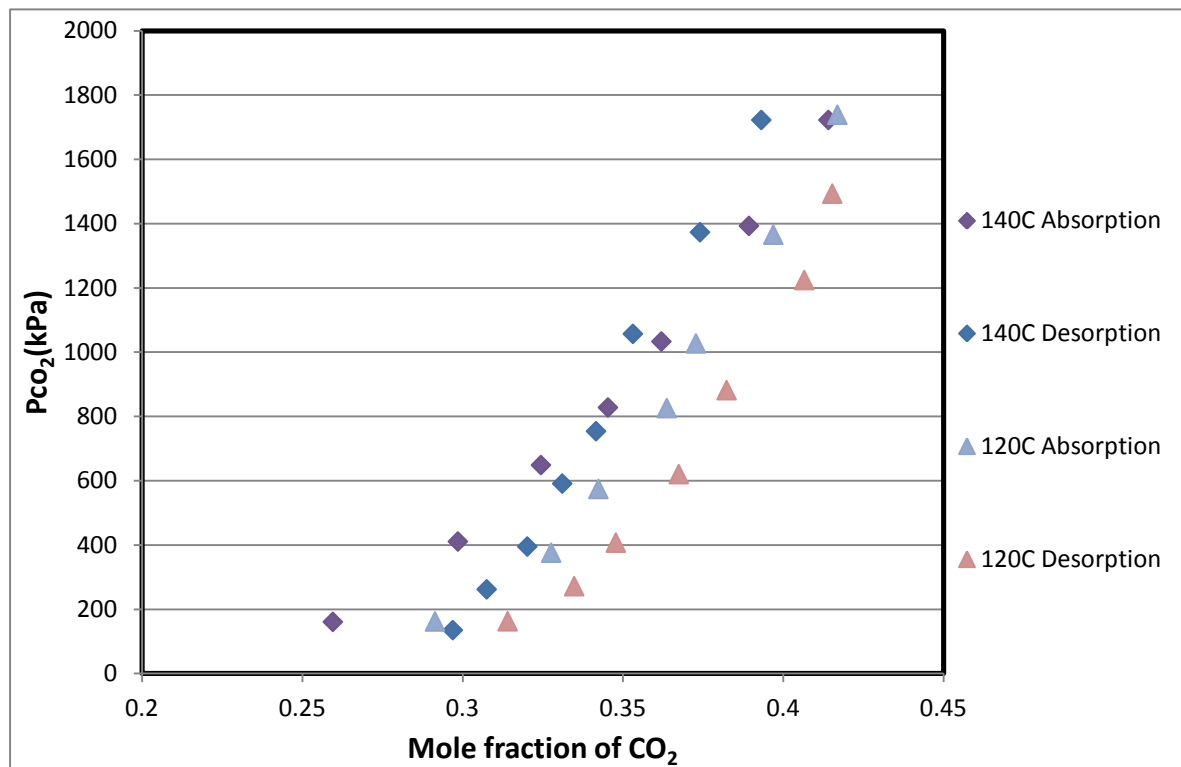


Figure 4.23. Additional experiment data of 0.7P₄₄₄₄Gly-0.3PEG400 at 120 °C and 140 °C

Easy to see, the curves for 120 °C lays between the curve of 100 °C and 140 °C, but the 120 °C curve is more closer to 140 °C curve. This means the absorption and desorption of 120 °C has not much difference, compared with the performance at 140 °C.

Also **Figure 4.24.** is a clear comparison of finished samples in 100 °C, 120 °C and 140 °C.



Figure 4.24. Comparison of 0.7P₄₄₄₄Gly-0.3PEG400 before experiment, after 100 °C, 120 °C and 140 °C experiment (from left to right)

Interestingly, there is almost no solid in 120 °C, implies an adequate desorbing process similar as 140 °C. But the colour change is not that big, just a few more than 100 °C.

Based on this two points, in 120 °C , the mixed system has very similar properties with 140 °C, but the negative decomposition is much lesser. Those results indicate 120 °C as a better temperature, thus recommended for the later research.

5. Discussions and Recommendations

5.1. Impurities of P₄₄₄₄Gly

Although the NMR result of produced P₄₄₄₄Gly is highly identical, indicates a very high purity to all products. However, there is observable colour difference between each samples. The relevant assumption is, the produced P₄₄₄₄Gly might decompose a bit during oven heating. Li's research (2014, pp.82) also shows that, the solution slightly lose weight after breezing by pure nitrogen for 300 minutes, which indicates the impurities might be volatile organic compounds. The samples for reference are shown in **Figure 5.1**.

Another issue is, even ionic liquids have low vapour pressure, some product still has a weak irritating odor, that is also unreasonable and those organic impurities is considered to be the reason.

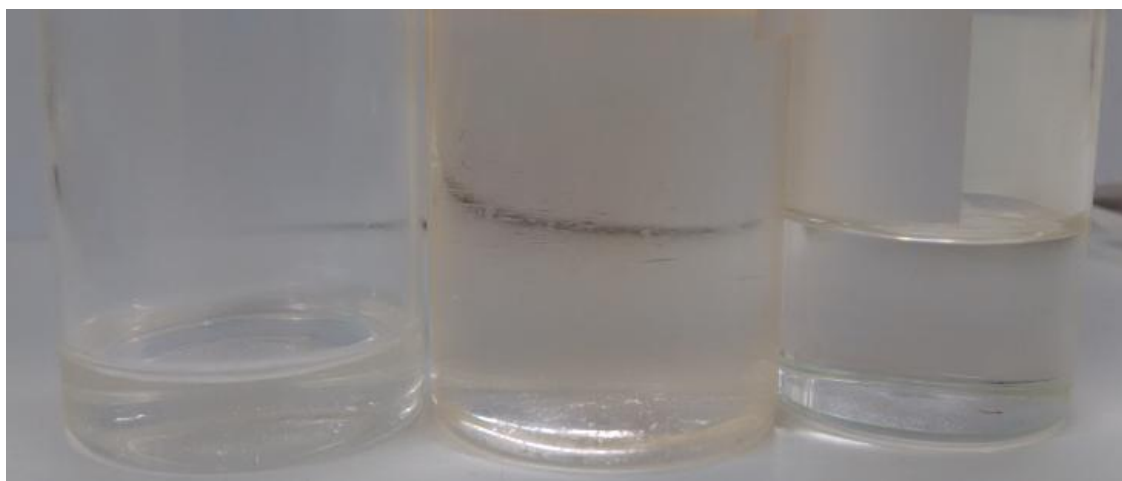


Figure 5.1. Slight colour difference between different samples

5.2. "Black Liquid" Issue in High Temperatures

According to the previous experiments, the solution became darker when temperature and concentration of P₄₄₄₄Gly is higher. Besides the above figures as reference, **Figure 5.2.** reveals the solution is darker when placing in high temperature (140 °C) for long time. This brings up this system a challenge of thermal resistance for further industrial use.

Since the decomposition temperature of P₄₄₄₄Gly is 165 °C (Cao & Mu, 2014), not far from 140 °C, implies that the solution might be metamorphic. Another idea from Uerdingen et al. (2005) advocate that the ionic liquid is corrosive and might react with the steel-made reaction vessel in that temperature. Combined with the result of Section 4.6., 140 °C is not a suggested temperature for this experiment.

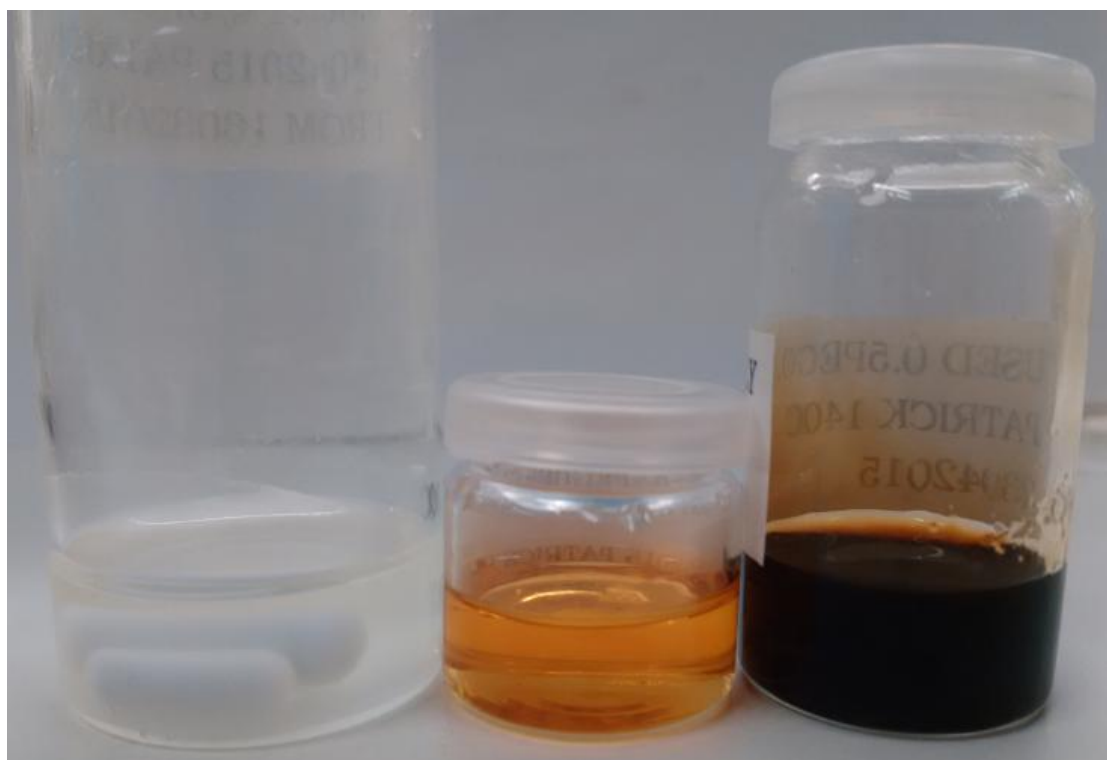


Figure 5.2. An comparison of produced 0.5P₄₄₄₄Gly-0.5PEG400 before experiment, after 140 °C experiment for 14 hours and after 140 °C experiment for 4-5 days (from left to right)

5.3. Comparison of Henry's Constant

The Section 3.6. shows the calculation method of Henry's constant with several examples. Since physical absorbent is easier to discuss, with excluding a little of abnormal figure (some data with similar number but one inside is strangely large/small), the figure of PEG400 can be compared with data from Li et al. (2011) and shown in **Table 5.1**. It is also necessary to point out that, the data of Li et al. (2011) is Henry's constant by molality, which is converted by the normal Henry's constant by molar fraction.

Table 5.1. Henry's constant of PEG400 with comparison

Temperature (°C)	Henry's Constant (MPa)		Difference (%)
	This work	Li et al. (2011)	
30		4.68 ±0.17	
40	5.02 ±0.79	5.62 ±0.33	11.95%
50		6.51 ±0.08	
60	5.98 ±0.80	6.99 ±0.27	16.89%
100	8.91 ±0.40		
140	10.77 ±0.81		

According to the above table, the Henry's constant range of this work is far larger than the literature value, and also the error of this work and literature can be mostly 16.89%. The result of this work is having a smaller Henry's constant than literature value indicating a potentially large absorption amount, the apparatus leakage is not very possible to happen. Still, the result can be referred for the comparison to other data.

For other mixtures with P₄₄₄₄Gly, the main absorption will be chemical absorption, the main character is a high absorption rate in the first point, then rapidly reduces in the following points, this comes to a very small Henry's constant at the beginning, then rapidly increases in the next several data. For a comprehensive evaluation of the absorption effect, an average Henry's constant will be calculated, with the highest difference of upper/lower range provided.

The rest, by the same theory, the rest figure of other mixtures can be analyzed in **Table 5.2**.

Table 5.2. Henry's constant of various P₄₄₄₄Gly-PEG400 blend

Temperature (°C)	Henry's Constant (MPa)		
	60	100	140

0.3P₄₄₄₄Gly-0.7PEG400	2.43 ± 2.14	3.13 ± 2.55	4.31 ± 2.22
0.5P₄₄₄₄Gly-0.5PEG400	2.32 ± 1.62	2.50 ± 1.82	2.46 ± 2.28
0.7P₄₄₄₄Gly-0.3PEG400	1.83 ± 1.40	1.99 ± 1.58	2.43 ± 1.81
P₄₄₄₄Gly	1.63 ± 1.50	1.64 ± 1.41	

Compared with *Table 3.2*. (Anthony et al., 2005), it is easy to find out that all blends is considered as relatively good solvent. Besides the figure of 0.5P₄₄₄₄Gly-0.5PEG400 in 140 °C is clearly abnormal, this graph had clearly shows, the Henry's constant decreases when temperature decreases and when ratio of P₄₄₄₄Gly increases. Among then, the range of constant becomes greater when temperature is lower or P₄₄₄₄Gly has higher concentration. Since a greater range and lower Henry's constant is desired, this analysis cannot give a clear suggestion. Hence, the suggestions on before sections remains.

6. Conclusion

In conclusion, this thesis aims for detailed studies of P₄₄₄₄Gly-PEG400 system, with a full assessment of synthesis of ionic liquid, density and viscosity test, solubility test, analysis and improvement.

As the prerequisite of the experiment, the synthesis of P₄₄₄₄Gly runs well, the NMR result shows a satisfied purity although there is slight colour difference. The density of all blends at 20-80 °C are measured and agrees with literature data, it is also perfectly linear, therefore a gradient of -0.0006 for P₄₄₄₄Gly and -0.0008 for PEG400 is applied. The viscosity of PEG400 and 0.3P₄₄₄₄Gly-0.7PEG400 are measured at 25-120 °C but with large errors as compares with literature values.

Carbon absorption experiment is the highlight point of this thesis, based on the former studies, PEG400, P₄₄₄₄Gly, and blends of 0.3P₄₄₄₄Gly-0.7PEG400, 0.5P₄₄₄₄Gly-0.5PEG400 and 0.7P₄₄₄₄Gly-0.3PEG400 are fully or partially tested at 40, 60, 100, 120, 140 °C, with detected Henry's constant range from 1.63-10.77 MPa. The 0.5P₄₄₄₄Gly-0.5PEG400 is most recommended of its highest cost efficiency, 0.3P₄₄₄₄Gly-0.7PEG400 is slightly inferior, but other blends are not recommended. As for temperature, it comes to be the best result when doing absorption at 60 °C and desorption at 120 °C. The analysis of Henry's constant related to different aspects, the best solution highly depends on what the experiment condition is.

The solution is getting deeper colour when having a higher temperature, this is more serious when temperature reaches 140 °C, thus a high temperature is always suitable to be avoided. The result of cyclic capacity revealed that, the differences between absorption and desorption after the second cycle are very little, therefore the circulated use of this absorbent is considered not efficient.

Lastly, a more comparative studies is recommended for better evaluation and finding a better solution of carbon capture, more detailed ratio and temperature is always useful for a fine adjustment. Further researches are useful, such as further studies of kinetics and mechanics could be useful for modeling and thus easier for more theoretical induction. Absorption is also a traditional method, as shown on the literature review, it is possible and potentially more effective when combining with membrane separation, an emerging and promising technology. All in all, the utilization of P₄₄₄₄Gly-PEG400 has a high potential and still waiting for further research and improvement.

7. References

Aaron, D., & Tsouris, C. (2005). Separation of CO₂ from flue gas: a review. *Separation Science and Technology*, 40(1-3), 321-348.

Anthony, J. L., Maginn, E. J., & Brennecke, J. F. (2002). Solubilities and thermodynamic properties of gases in the ionic liquid 1-n-butyl-3-methylimidazolium hexafluorophosphate. *The Journal of Physical Chemistry B*, 106(29), 7315-7320.

Aschenbrenner, O., & Styring, P. (2010). Comparative study of solvent properties for carbon dioxide absorption. *Energy & Environmental Science*, 3(8), 1106-1113.

Benemann, J. R. (1997). CO₂ mitigation with microalgae systems. *Energy conversion and management*, 38, S475-S479.

Bernardo, P., Drioli, E., & Golemme, G. (2009). Membrane gas separation: a review/state of the art. *Industrial & Engineering Chemistry Research*, 48(10), 4638-4663.

Blanchard, L. A., Hancu, D., Beckman, E. J., & Brennecke, J. F. (1999). Green processing using ionic liquids and CO₂. *Nature*, 399(6731), 28-29.

Cadena, C., Anthony, J. L., Shah, J. K., Morrow, T. I., Brennecke, J. F., & Maginn, E. J. (2004). Why is CO₂ so soluble in imidazolium-based ionic liquids?. *Journal of the American Chemical Society*, 126(16), 5300-5308.

Cao, Y., & Mu, T. (2014). Comprehensive investigation on the thermal stability of 66 ionic liquids by thermogravimetric analysis. *Industrial & Engineering Chemistry Research*, 53(20), 8651-8664.

Chen J., Spear S. K., Huddleston J. G., Rogers R. D. (2007). Polyethylene glycol and solutions of polyethylene glycol as green reaction media[J]. *Green Chemistry*, 7(2), 64-82.

D'Alessandro, D. M., Smit, B., & Long, J. R. (2010). Carbon dioxide capture: prospects for new materials. *Angewandte Chemie International Edition*, 49(35), 6058-6082.

Dewulf, J., Drijvers, D., & Van Langenhove, H. (1995). Measurement of Henry's law constant as function of temperature and salinity for the low temperature range. *Atmospheric Environment*, 29(3), 323-331.

Eliassi, A., Modarress, H., & Mansoori, G. A. (1998). Densities of poly (ethylene glycol)+ water mixtures in the 298.15-328.15 K temperature range. *Journal of Chemical & Engineering Data*, 43(5), 719-721.

Francisco, G. J. (2006). Separation of carbon dioxide from nitrogen using poly (vinyl alcohol)-amine blend membranes (Doctoral dissertation, University of Waterloo).

Gourgouillon, D., Avelino, H. M. N. T., Fareleira, J. M. N. A., & Da Ponte, M. N. (1998). Simultaneous viscosity and density measurement of supercritical CO₂-saturated PEG 400. *The Journal of supercritical fluids*, 13(1), 177-185.

Gui, X., Tang, Z., & Fei, W. (2010). CO₂ capture with physical solvent dimethyl carbonate at high pressures. *Journal of Chemical & Engineering Data*, 55(9), 3736-3741.

Han, F., Zhang, J., Chen, G., Wei, X. (2008). Density, Viscosity, and Excess Properties for Aqueous Poly(ethylene glycol) Solutions from (298.15 to 323.15) K. *Journal of Chemical & Engineering Data*, 53(11), 2598-2601.

Hasib-ur-Rahman, M., Sijaj, M., & Larachi, F. (2010). Ionic liquids for CO₂ capture—development and progress. *Chemical Engineering and Processing: Process Intensification*, 49(4), 313-322.

Hossain, M. M., & de Lasa, H. I. (2008). Chemical-looping combustion (CLC) for inherent CO₂ separations—a review. *Chemical Engineering Science*, 63(18), 4433-4451.

Huang, J., & Rüther, T. (2009). Why are ionic liquids attractive for CO₂ absorption? An overview. *Australian journal of chemistry*, 62(4), 298-308.

Jerome, F. S., Tseng, J. T., & Fan, L. T. (1968). Viscosities of aqueous glycol solutions. *Journal of Chemical & Engineering Data*, 13(4), 496-496.

H. Davis, Jr, J. (2004). Task-specific ionic liquids. *Chemistry letters*, 33(9), 1072-1077.

Kasahara, S., Kamio, E., Otani, A., & Matsuyama, H. (2014). Fundamental Investigation of the Factors Controlling the CO₂ Permeability of Facilitated Transport Membranes Containing Amine-Functionalized Task-Specific Ionic Liquids. *Industrial & Engineering Chemistry Research*, 53(6), 2422-2431.

Li, J. (2014). Intensification of CO₂ capture by mixed solvent systems based on alkanolamines or ionic liquids with polyethylene glycols as co-solvent. Ph.D Thesis, East China University of Science and Technology: Shanghai.

Li, J., Ye, Y., Chen, L., & Qi, Z. (2011). Solubilities of CO₂ in Poly (ethylene glycols) from (303.15 to 333.15) K. *Journal of Chemical & Engineering Data*, 57(2), 610-616.

Lin, J., Ding, Z., Hou, Y., & Wang, X. (2013). Ionic Liquid Co-catalyzed Artificial Photosynthesis of CO. *Scientific Reports*, 3.

Murdock, J. W. (1993). *Fundamental fluid mechanics for the practicing engineer*. CRC Press.

Ottani, S., Vitalini, D., Comelli, F., & Castellari, C. (2002). Densities, viscosities, and refractive indices of poly (ethylene glycol) 200 and 400+ cyclic ethers at 303.15 K. *Journal of Chemical & Engineering Data*, 47(5), 1197-1204.

Peng, J., & Deng, Y. (2001). Cycloaddition of carbon dioxide to propylene oxide catalyzed by ionic liquids. *New Journal of Chemistry*, 25(4), 639-641.

Perissi, I., Bardi, U., Caporali, S., & Lavacchi, A. (2006). High temperature corrosion properties of ionic liquids. *Corrosion science*, 48(9), 2349-2362.

Rao, A. B., & Rubin, E. S. (2002). A technical, economic, and environmental assessment of amine-based CO₂ capture technology for power plant greenhouse gas control. *Environmental science & technology*, 36(20), 4467-4475.

Raupach, M. R., Marland, G., Ciais, P., Le Qué^e C., Canadell, J. G., Klepper, G., & Field, C. B. (2007). Global and regional drivers of accelerating CO₂ emissions. *Proceedings of the National Academy of Sciences*, 104(24), 10288-10293.

Redlich, O., & Kwong, J. N. (1949). On the thermodynamics of solutions. V. An equation of state. Fugacities of gaseous solutions. *Chemical reviews*, 44(1), 233-244.

Rochelle, G. T. (2009). Amine scrubbing for CO₂ capture. *Science*, 325(5948), 1652-1654.

Romero, A., Santos, A., Tojo, J., & Rodriguez, A. (2008). Toxicity and biodegradability of imidazolium ionic liquids. *Journal of Hazardous*

Materials, 151(1), 268-273.

Rooney, D., Jacquemin, J., & Gardas, R. (2010). Thermophysical properties of ionic liquids. In *Ionic Liquids* (pp. 185-212). Springer Berlin Heidelberg.

Trivedi, S., Bhanot, C., & Pandey, S. (2010). Densities of {poly (ethylene glycol)+ water} over the temperature range (283.15 to 363.15) K. *The Journal of Chemical Thermodynamics*, 42(11), 1367-1371.

Seddon, K. R. (1997). Ionic liquids for clean technology. *Journal of Chemical Technology and Biotechnology*, 68(4), 351-356.

Uerdingen, M., Treber, C., Balsler, M., Schmitt, G., & Werner, C. (2005). Corrosion behaviour of ionic liquids. *Green Chemistry*, 7(5), 321-325.

Usman, M. (2012). Kinetics study of CO₂ absorption in AMP and PZ solutions. MSc Thesis, Norwegian University of Science and Technology: Trondheim.

Veawab, A., Tontiwachwuthikul, P., & Chakma, A. (1999). Corrosion behavior of carbon steel in the CO₂ absorption process using aqueous amine solutions. *Industrial & engineering chemistry research*, 38(10), 3917-3924.

Wang, W., Yang, X., Fang, Y., Ding, J., & Yan, J. (2009). Preparation and thermal properties of polyethylene glycol/expanded graphite blends for energy storage. *Applied Energy*, 86(9), 1479-1483.

Wasserscheid, P., & Keim, W. (2000). Ionic liquids-new " solutions" for transition metal catalysis. *Angewandte Chemie*, 39(21), 3772-3789.

Wu, T. Y., Wang, H. C., Su, S. G., Gung, S. T., Lin, M. W., & Lin, C. B. (2010). Characterization of ionic conductivity, viscosity, density, and self-diffusion coefficient for binary mixtures of polyethyleneglycol (or polyethyleneimine) organic solvent with room temperature ionic liquid BMIBF 4 (or BMIPF 6). *Journal of the Taiwan Institute of Chemical Engineers*, 41(3), 315-325.

Yang, H., Xu, Z., Fan, M., Gupta, R., Slimane, R. B., Bland, A. E., & Wright, I. (2008). Progress in carbon dioxide separation and capture: A review. *Journal of Environmental Sciences*, 20(1), 14-27.

Yoshizawa, M., Xu, W., & Angell, C. A. (2003). Ionic liquids by proton transfer: Vapor pressure, conductivity, and the relevance of $\Delta p K_a$ from aqueous solutions. *Journal of the American Chemical Society*, 125(50),

15411-15419.

Zanganeh, K. E., Shafeen, A., & Salvador, C. (2009). CO₂ capture and development of an advanced pilot-scale cryogenic separation and compression unit. *Energy Procedia*, 1(1), 247-252.

Zhang, J., Zhang, S., Dong, K., Zhang, Y., Shen, Y., & Lv, X. (2006). Supported absorption of CO₂ by tetrabutylphosphonium amino acid ionic liquids. *Chemistry-A European Journal*, 12(15), 4021-4026.

8. Appendices

Appendix I. NMR spectrometer, Bruker/Oxford DPX 400 MHz



Appendix II. Density meter, Anton Paar DMA 4500M (Usman, 2012)



Appendix III. Rheometer, TA Instruments Discovery HR-2



Appendix IV. Evaporator

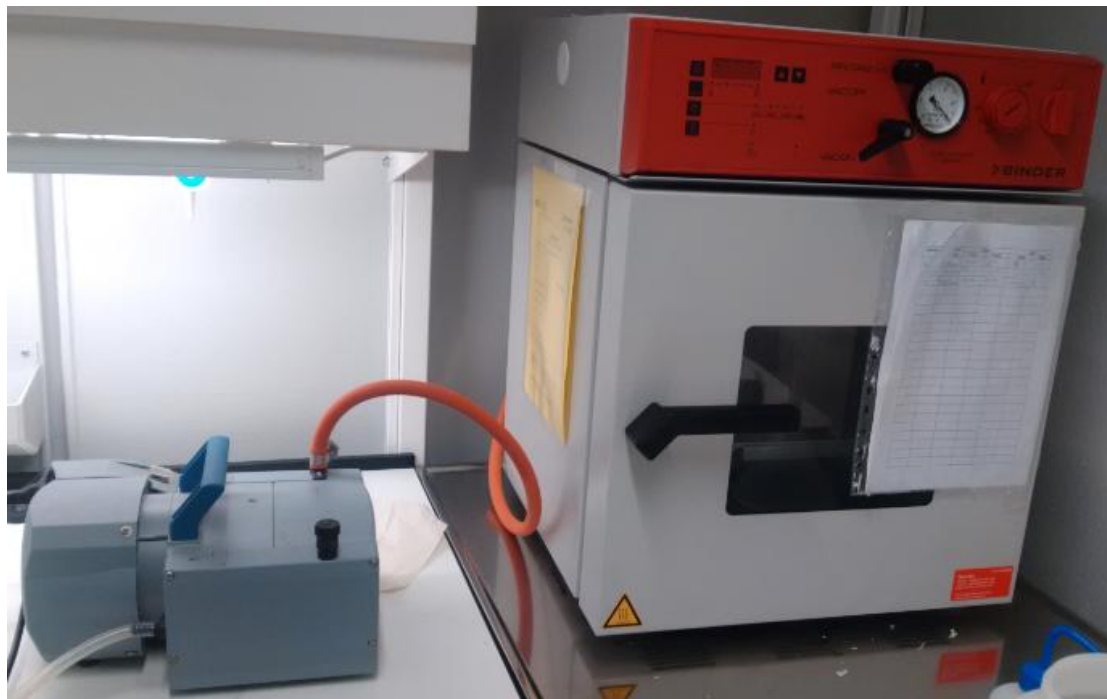
The evaporator is assembled by MEMFO, and the following figure shows the graphical detail of the evaporator.



The main part of evaporator is on the middle, which holds the distillation flask and connect it to the waste container for evaporated liquids. There are also silicone oil for oil bath, heater and stirrer for heating and stirring, vacuum pump for making vacuum, in order to decrease the boiling point, as well as a tap to provide water for cooling and condensation.

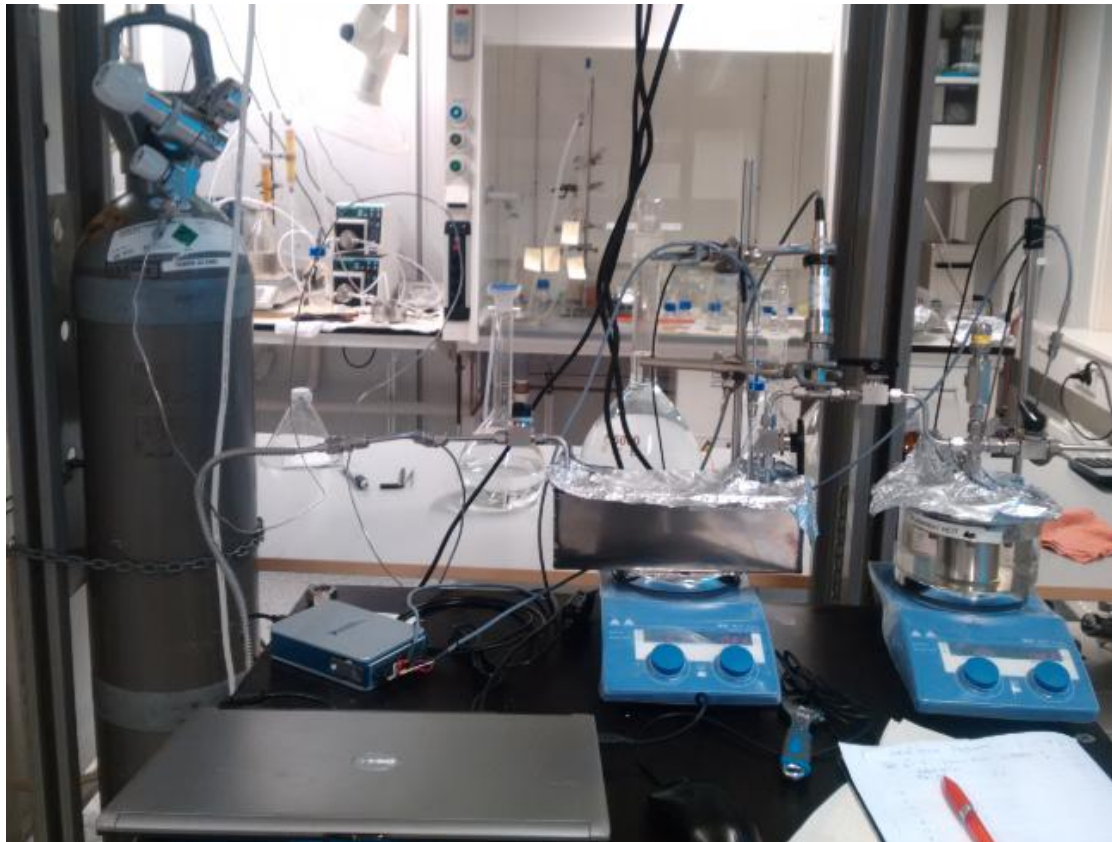
Appendix V. Vacuum oven

The vacuum oven is assembled by MEMFO, and the following figure shows the graphical detail of the oven.

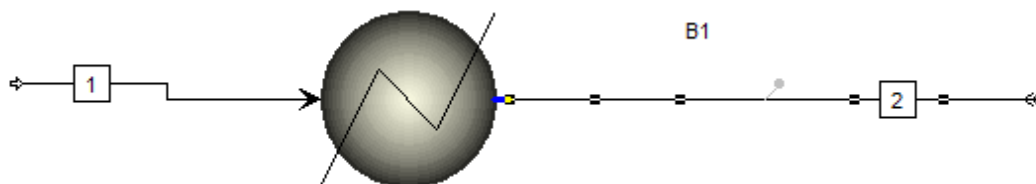


The well-sealed oven could fully separate the inner chemical to outside environment, a vacuum pump is linked to pump out the air inside, and the temperature inside can be set for heating purposes.

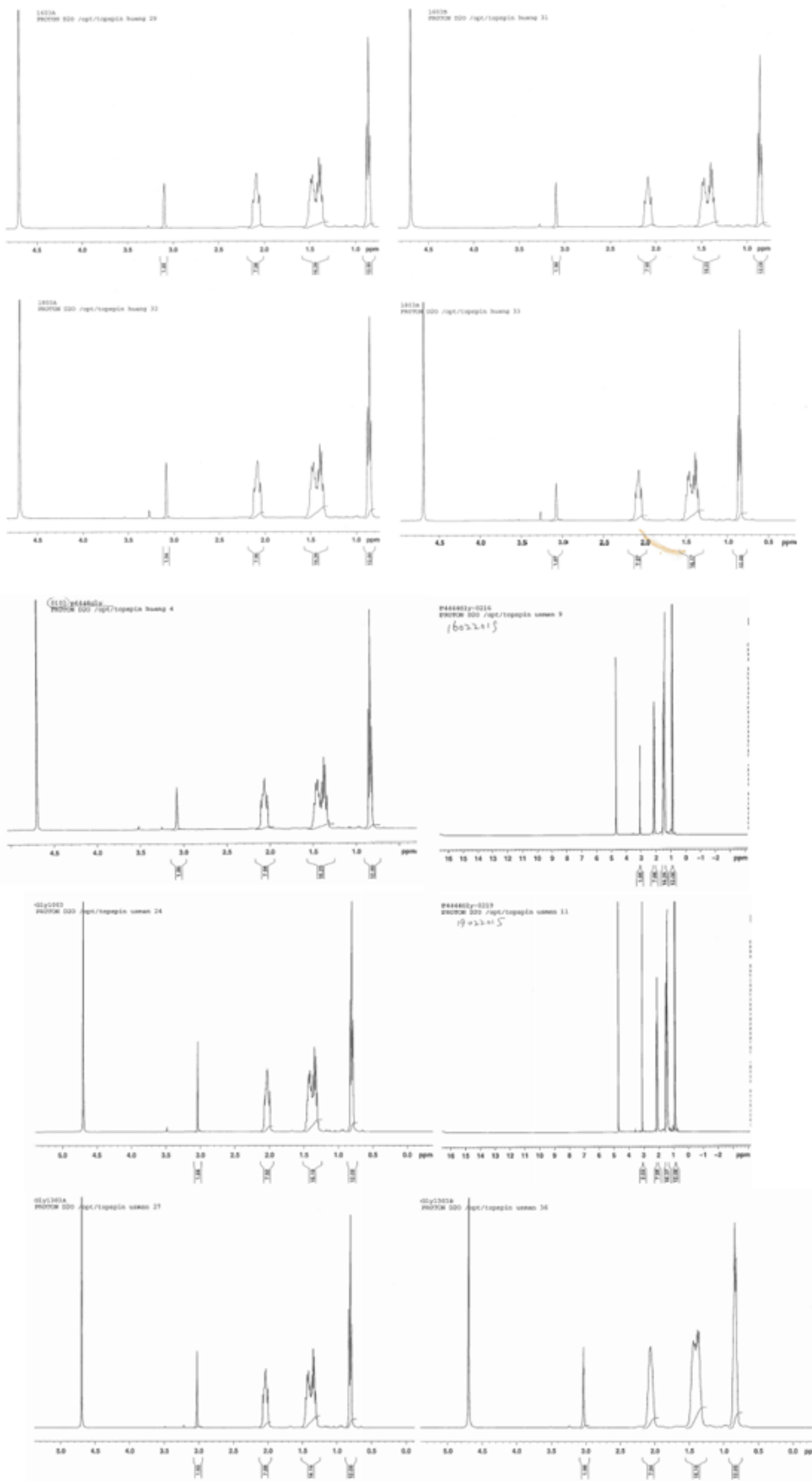
Appendix VI. Solubility of CO₂ in PEGs



Appendix VII. CO₂ calculation by Aspen Plus V8.2, simulator part



Appendix VIII. Various NMR result graphs



Appendix IX. CO₂ calculation by Aspen Plus V8.2, result page

Material	Vol.% Curves	Wt. % Curves	Petroleum	Polymers	Solids	Status
Display: Streams Format: FULL Stream Table						
		1				
▶ Substream: MIXED						
▶ Mole Flow kmol/hr						
▶ 1		0.0422037				
▶ Total Flow kmol/hr		0.0422037				
▶ Total Flow kg/hr		1.85738				
▶ Total Flow l/min		1.81176				
▶ Temperature C		140				
▶ Pressure kPa		1308				
▶ Vapor Frac		1				
▶ Liquid Frac		0				
▶ Solid Frac		0				
▶ Enthalpy cal/mol		-92963.3				
▶ Enthalpy cal/gm		-2112.33				
▶ Enthalpy cal/sec		-1089.83				
▶ Entropy cal/mol-K		-1.42631				
▶ Entropy cal/gm-K		-0.0324088				
▶ Density mol/cc		0.000388239				
▶ Density gm/cc		0.0170863				
▶ Average MW		44.0098				
▶ Liq Vol 60F l/min		0.0376723				

Appendix X. Density of PEG400, P₄₄₄₄Gly and their blends

Component	Density (g/cm ³)				
	20 °C	30 °C	40 °C	60 °C	80 °C
De-ionized Water	0.9982	0.99564	0.99223	0.98306	0.95891
PEG400	1.12613	1.11784	1.10938	1.09332	1.07707
0.3P₄₄₄₄Gly-0.7PEG400	1.07505	1.06789	1.06077	1.04658	1.03242
0.5P₄₄₄₄Gly-0.5PEG400	1.04282	1.03608	1.02938	1.01553	1.00213
0.7P₄₄₄₄Gly-0.3PEG400	1.01196	1.00561	0.99929	0.98669	-
P₄₄₄₄Gly	0.96585	0.96014	0.95403	0.94198	0.92999

Appendix XI. Density comparison of PEG400

Component	Density of PEG400 (g/cm ³)				
	20 °C	30 °C	40 °C	60 °C	80 °C
This work	1.12613	1.11784	1.10938	1.09332	1.07707
Han et al.		1.1180	1.1097		
Trivedi et al.	1.1265	1.1181	1.1098	1.0962	1.0833
Eliassi et al.			1.1102		
Wu et al.			1.1122	1.0973	1.0815

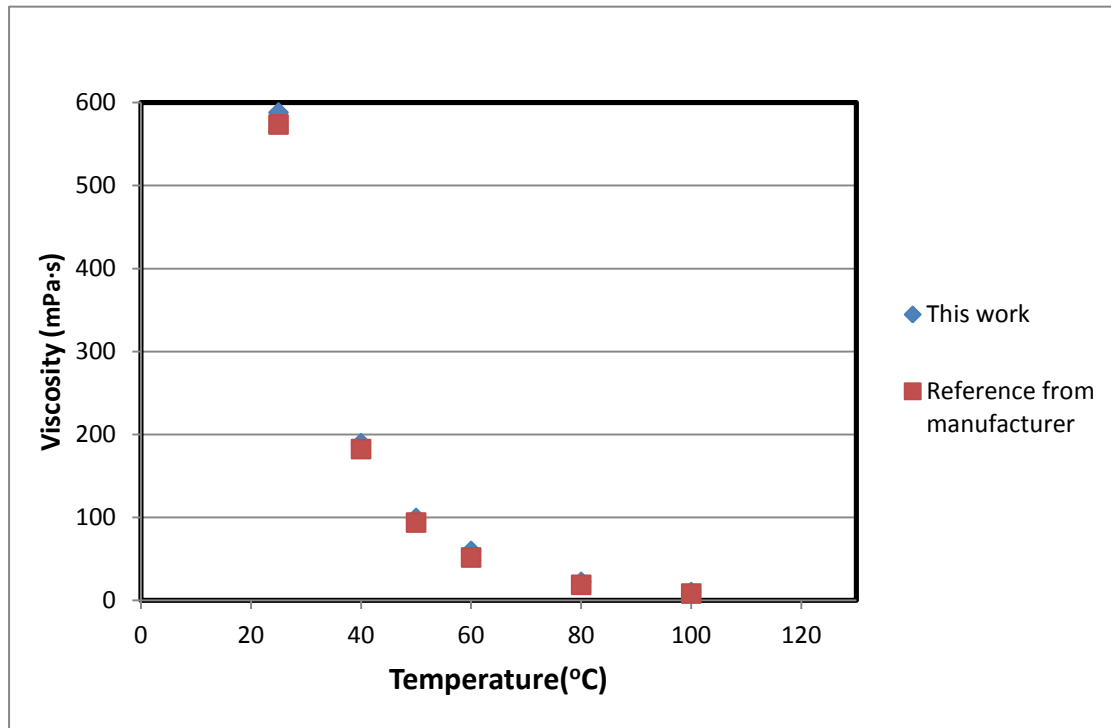
Appendix XII. Viscosity data of PEG400 and 0.3P₄₄₄₄Gly-0.7PEG400

Temperature	Viscosity of Component (mPa s)	
	PEG400	0.3P ₄₄₄₄ Gly-0.7PEG400
25 °C	99.17	162.7
40 °C	49.18	75.50
45 °C	45.00	
50 °C	34.45	
60 °C	26.74	38.11
80 °C	16.56	26.10
100 °C	11.40	21.23
120 °C	8.657	15.53

Appendix XIII. Comparison of PEG400 viscosity

Temperature	Various viscosities (mPa s)					
	This work	Han et al.	Wu et al.	Ottani et al.	Jerome et al.	Gourgouillon et al.
25 °C	99.17	94.4		92.797	99.01	
30 °C		69.1		71.776		
35 °C		55.6	58.19	59.406		
40 °C	49.18	44.4	48.38			44.46
45 °C	45.00	34.2	38.79			
50 °C	34.45	25.7	33.81			
60 °C	26.74		23.4			
80 °C	16.56		12.71			
100 °C	11.40					
120 °C	8.657					

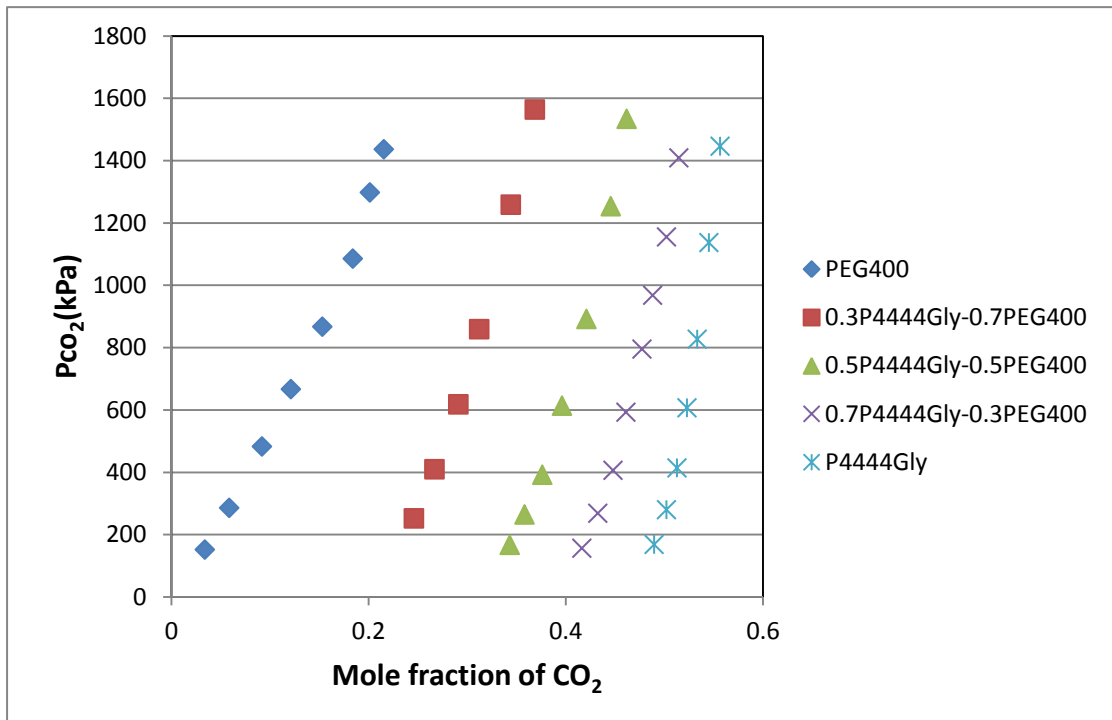
Appendix XIV. Viscosity difference between this rheometer and reference



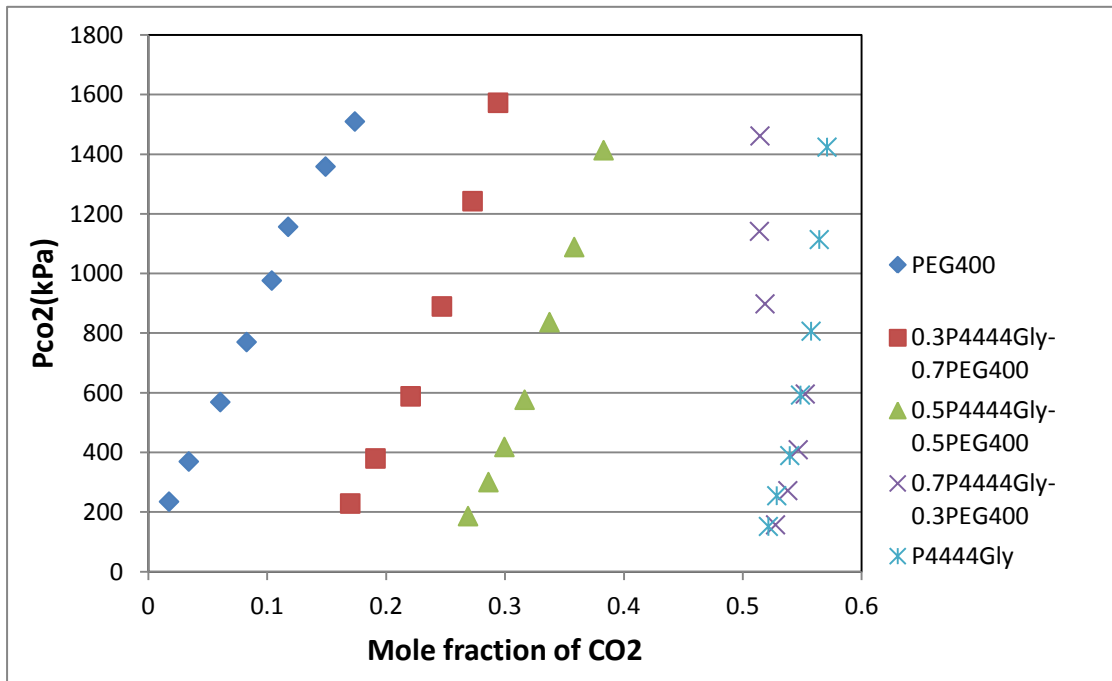
Appendix XV. Experimental Values of Mole Fraction and Molality of CO₂ in PEG400 at Equilibrium Pressure and Temperature (Li et al., 2011)

T	p		m_{CO_2}
K	kPa	x_{CO_2}	mol·kg ⁻¹
303.15	145.3	0.0319 ± 0.0001	0.0822 ± 0.0003
	282.2	0.0622 ± 0.0002	0.1660 ± 0.0005
	431.2	0.0897 ± 0.0003	0.2464 ± 0.0007
	561.5	0.1244 ± 0.0003	0.3553 ± 0.0009
	815.5	0.1684 ± 0.0004	0.5063 ± 0.0013
	1070.0	0.2220 ± 0.0006	0.7134 ± 0.0018
313.15	166.0	0.0279 ± 0.0001	0.0717 ± 0.0003
	300.5	0.0567 ± 0.0002	0.1504 ± 0.0005
	414.4	0.0759 ± 0.0002	0.2054 ± 0.0007
	578.0	0.1027 ± 0.0003	0.2861 ± 0.0009
	834.5	0.1467 ± 0.0004	0.4298 ± 0.0013
	1087.5	0.1905 ± 0.0006	0.5885 ± 0.0017
323.15	154.1	0.0237 ± 0.0001	0.0607 ± 0.0003
	217.4	0.0333 ± 0.0001	0.0861 ± 0.0004
	443.0	0.0690 ± 0.0003	0.1854 ± 0.0007
	564.0	0.0877 ± 0.0003	0.2404 ± 0.0008
	893.8	0.1362 ± 0.0004	0.3942 ± 0.0013
	1120.5	0.1701 ± 0.0006	0.5125 ± 0.0017
333.15	147.8	0.0213 ± 0.0001	0.0544 ± 0.0003
	282.9	0.0421 ± 0.0002	0.1099 ± 0.0004
	434.5	0.0625 ± 0.0002	0.1666 ± 0.0006
	557.2	0.0775 ± 0.0003	0.2099 ± 0.0008
	831.0	0.1184 ± 0.0004	0.3356 ± 0.0012
	1104.0	0.1545 ± 0.0005	0.4567 ± 0.0016

Appendix XVI. CO₂ desorption data at 60 °C



Appendix XVII. CO₂ desorption data at 100 °C



Appendix XVIII. CO₂ desorption data at 140 °C

